

Chymotrypsin activity signals to intestinal epithelium by Protease-Activated Receptor-dependent mechanisms

Simon Guignard¹, Mahmoud Saifeddine², Koichiro Mihara², Majid Motahhary², Magali Savignac³, Laura Guiraud¹, David Sagnat¹, mireille sebbag⁴, Sokchea Khou¹, Corinne Rolland⁵, Barbara Bournet⁶, Louis Buscail⁶, Etienne Buscail¹, Laurent Alric⁷, Caroline Camare⁸, Mouna Ambli¹, Nathalie Vergnolle¹, Morley Hollenberg⁹, Celine Deraison¹, and Chrystelle Bonnart¹

¹Inserm U1220

²University of Calgary

³Toulouse Institute for Infectious and Inflammatory Diseases (Infinity) INSERM UMR1291

⁴INSERM UMR 1220

⁵INSERM

⁶Gastroenterology department Toulouse university Hospital

⁷Toulouse University Department of Internal Medicine and Digestive Diseases, Rangueil, Toulouse 3 University Hospital, Toulouse, France.

⁸Toulouse University Hospitals, Department of Clinical Biochemistry, Toulouse, France

⁹University of Calgary

June 30, 2023

Abstract

Background and purpose Chymotrypsin is a serine protease produced by the pancreas and secreted into the lumen of the small intestine, where it digests food proteins. Due to its presence in the gut lumen, we hypothesized that chymotrypsin activity may be found close to epithelial cells and signals to them via Protease-activated receptors (PARs). We deciphered molecular pharmacology mechanisms for chymotrypsin signaling in intestinal epithelial cells. **Experimental approaches** The presence and activity of chymotrypsin were evaluated by western blot (WB) and enzymatic activity tests in luminal and mucosal compartments of murine and human gut samples. The ability of chymotrypsin to cleave the extracellular domain of PAR1 or PAR2 was assessed using cell lines expressing N-terminally-tagged receptors. The cleavage site of chymotrypsin on PAR1 and PAR2 was determined by HPLC-MS analysis. To study the pharmacology of chymotrypsin signals, we investigated calcium signaling and ERK1/2 activation using calcium mobilization assays and WB in CMT93 intestinal epithelial cells. **Key results** We found that chymotrypsin was present and active in the vicinity of the murine and human colonic epithelium. Molecular pharmacology studies evidenced that chymotrypsin cleaved both PARs receptors. While chymotrypsin activated calcium and ERK1/2 signaling pathways through PAR2, it disarmed PAR1, preventing further activation by its canonical agonist thrombin. **CONCLUSION** Our work suggests that the function of chymotrypsin in the gut lumen goes well beyond a simple digestive role. Our results highlight the ability of chymotrypsin to signal to intestinal epithelial cells via PARs, which may have important physiological consequences in gut homeostasis.

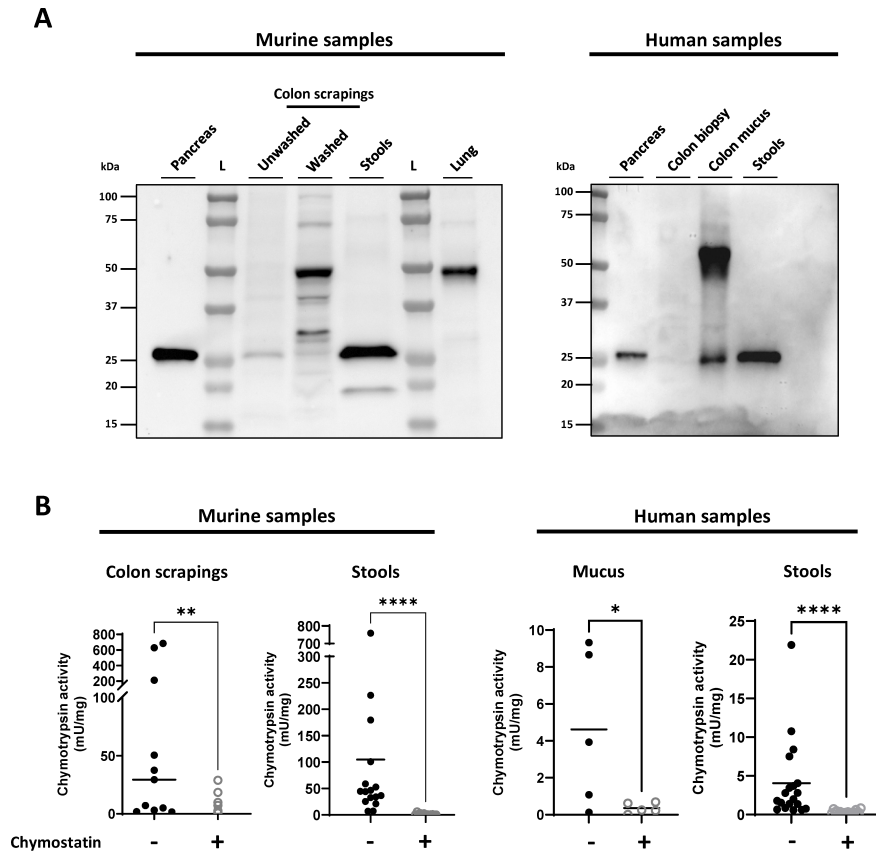


Figure 1. The colonic epithelium is exposed to chymotrypsin activity.

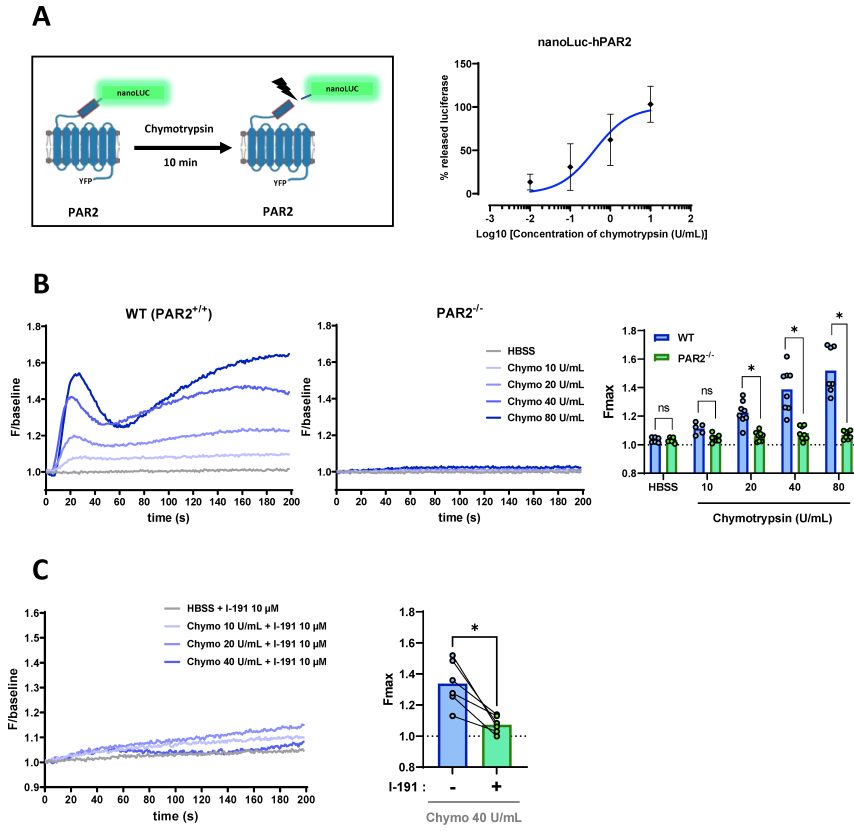


Figure 2. Chymotrypsin cleaves PAR2 and induces calcium signaling in CMT93 intestinal epithelial cells.

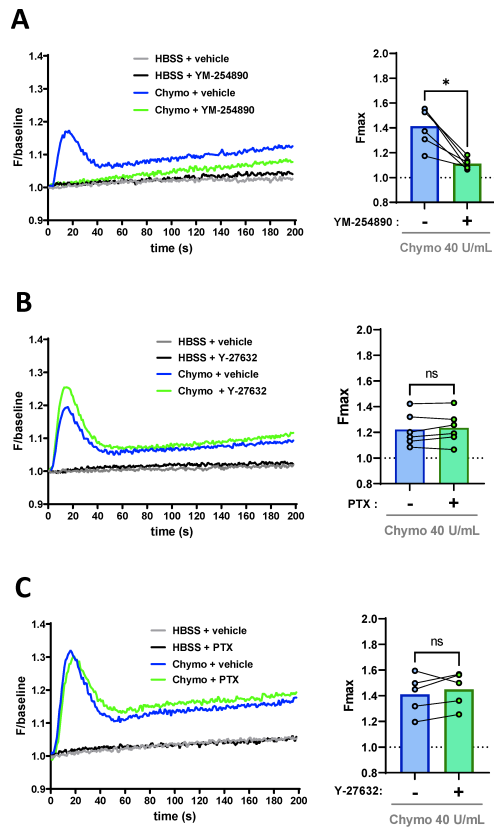


Figure 3. $G_{\alpha q}$ proteins, but not $G_{\alpha 12/13}$ nor $G_{\alpha i}$ proteins are involved in the calcium signal downstream PAR2 activation by chymotrypsin in CMT93 cells.

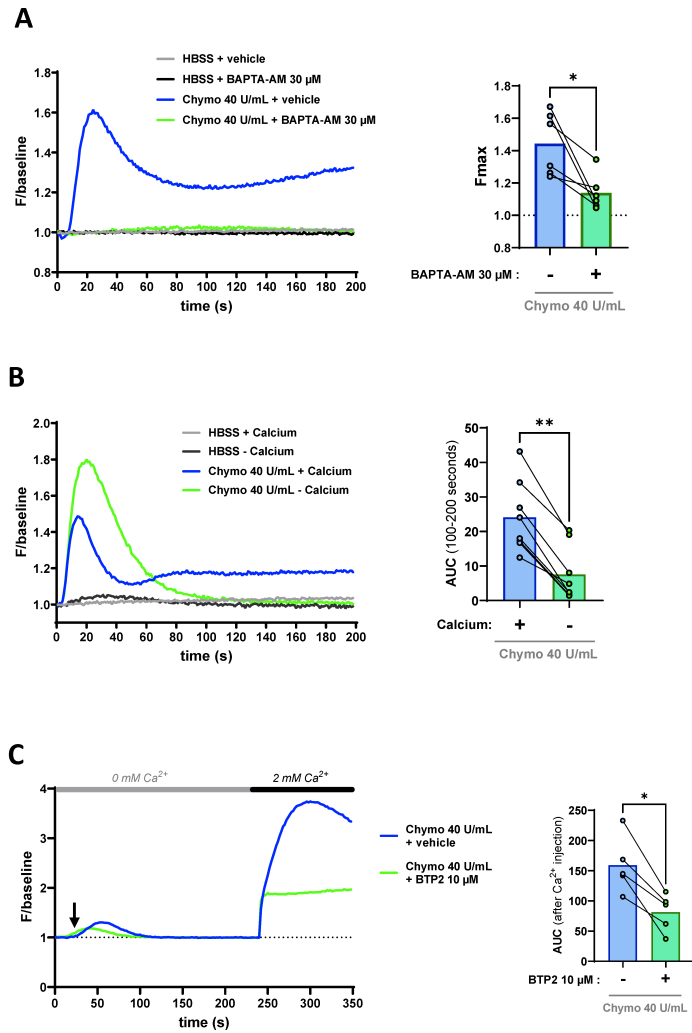


Figure 4. CRAC channels are involved in the long-term calcium influx observed downstream of PAR2 activation by chymotrypsin in CMT93 cells.

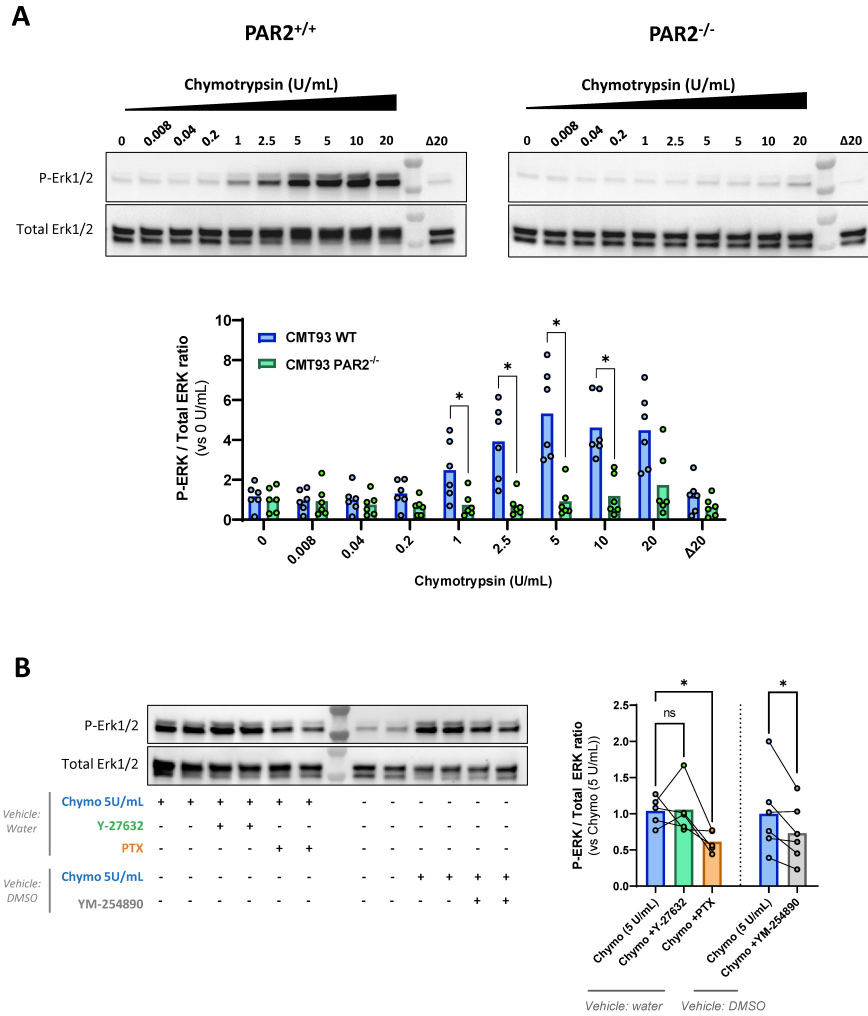


Figure 5. Chymotrypsin activates ERK1/2 signaling pathway via PAR2, depending on Gαq and Gαi proteins in intestinal epithelial cells.

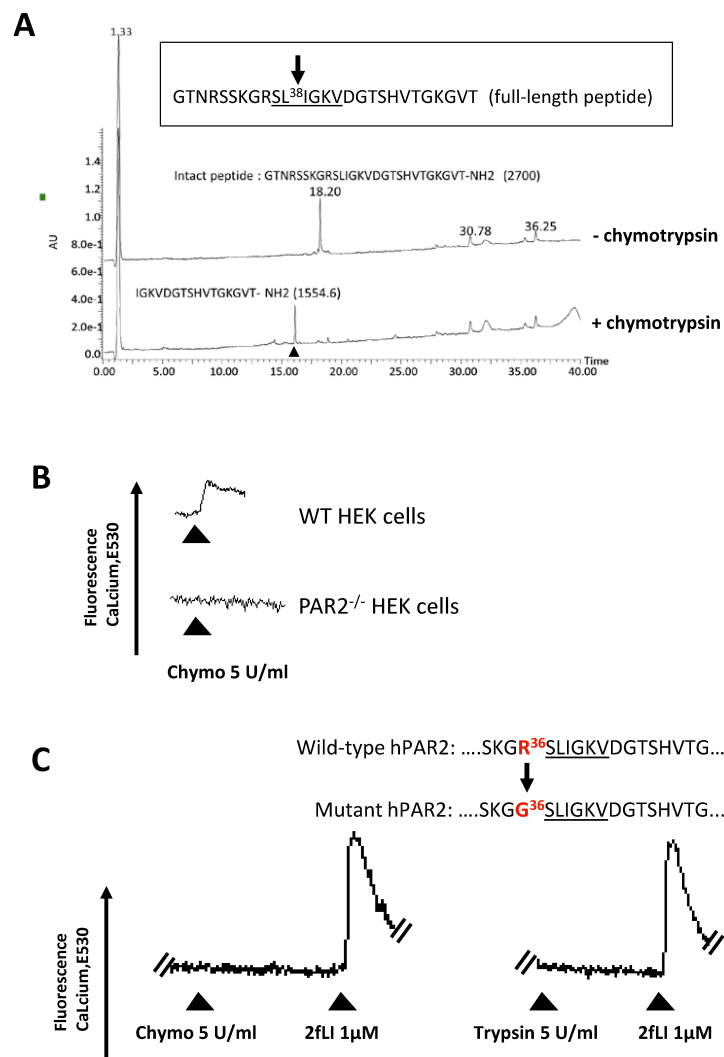


Figure 6. Chymotrypsin cleaves PAR2 at L³⁸/I³⁹ site *in vitro* but the canonical R³⁶/S³⁷ site may drive calcium signaling *in cellulo*.

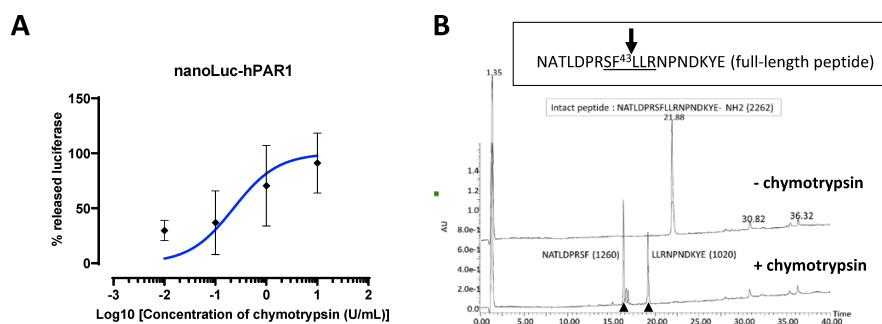


Figure 7. Chymotrypsin cleaves PAR1 N-terminal extremity

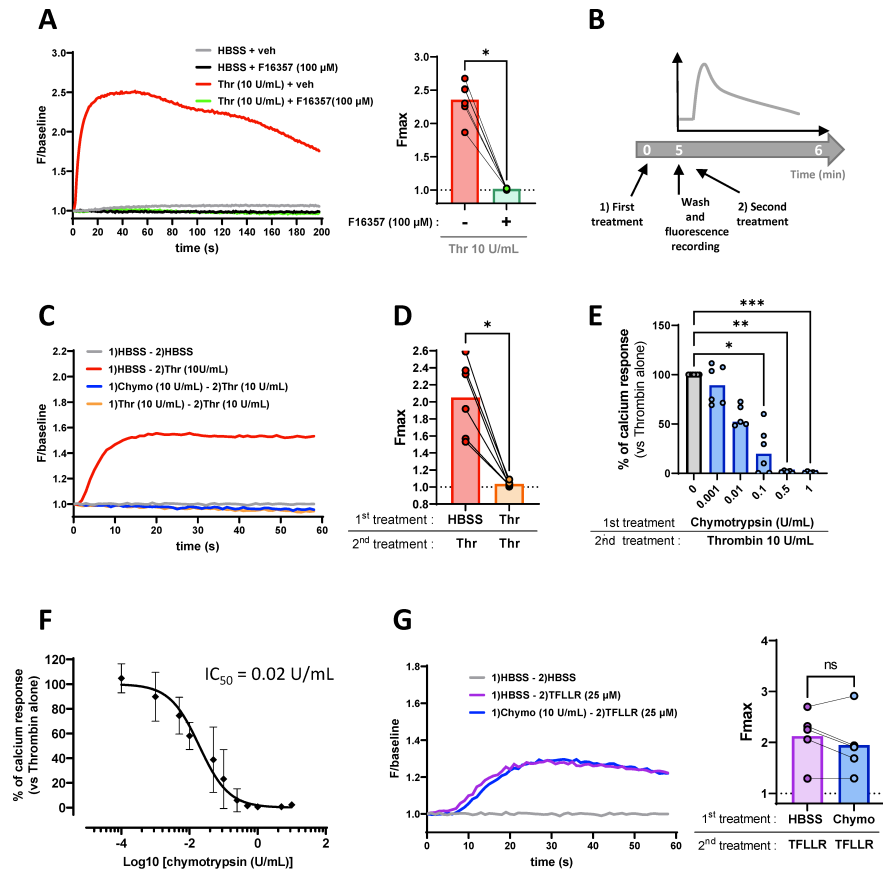


Figure 8. Chymotrypsin disarms PAR1 in intestinal epithelial cells

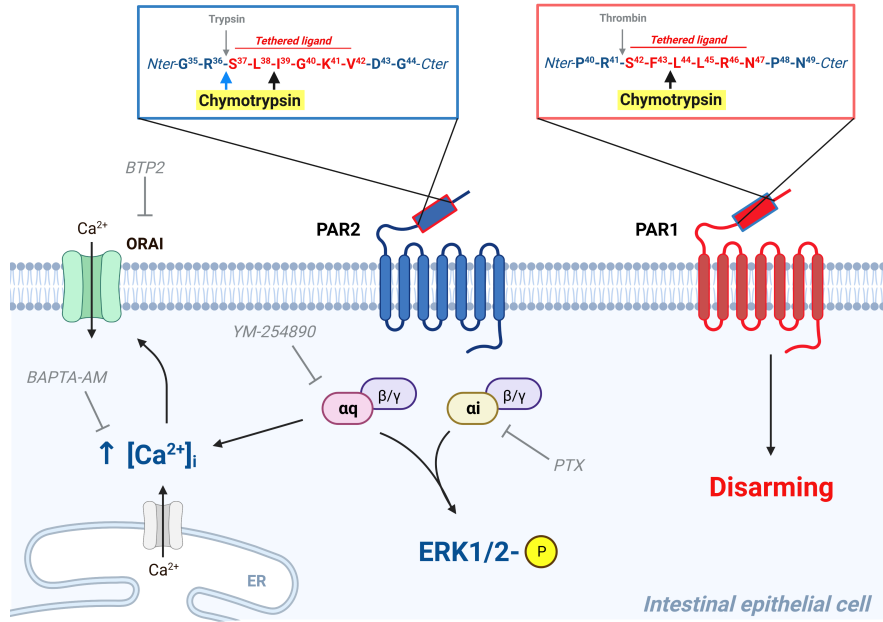


Figure 9. Schematic representation of chymotrypsin interactions with PAR1 and PAR2 at the surface of intestinal epithelial cells CMT93.

Chymotrypsin activity signals to intestinal epithelium by Protease-Activated Receptor-dependent mechanisms

Running title: Chymotrypsin signals through Protease-Activated Receptors

Simon Guignard¹, Mahmoud Saifeddine², Koichiro Mihara², Majid Motahhary², Magali Savignac³, Laura Guiraud¹, David Sagnat¹, Mireille Sebbag¹, Sokchea Khou¹, Corinne Rolland¹, Barbara Bournet⁴, Louis Buscail⁴, Etienne Buscail^{1,5}, Laurent Alric⁶, Caroline Camare^{7,8}, Mouna Ambli¹, Nathalie Vergnolle^{1,2,5}, Morley D. Hollenberg², Céline Deraison¹ and Chrystelle Bonnard¹

¹ *IRSD, Université de Toulouse, INSERM, INRAE, ENVT, Univ Toulouse III - Paul Sabatier (UPS), Toulouse, France*

² *Departments of Physiology & Pharmacology, and Medicine, University of Calgary Cumming School of Medicine, 3330 Hospital Drive NW, Calgary, Ab T2N 4N1, Canada.*

³ *Toulouse Institute for Infectious and Inflammatory Diseases (Infinity) INSERM UMR1291 - Centre National de la Recherche Scientifique UMR5051, University Paul Sabatier Toulouse III, F-31024 Toulouse, France*

⁴ *Gastroenterology department Toulouse university Hospital*

⁵ *Digestive surgery department Toulouse university Hospital*

⁶ *Toulouse University Department of Internal Medicine and Digestive Diseases, Rangueil, Toulouse 3 University Hospital, Toulouse, France.*

⁷ *Toulouse University Hospitals, Department of Clinical Biochemistry, Toulouse, France*

⁸ *University of Toulouse, UMR1297, Inserm/Paul Sabatier University, Toulouse, France*

§Address for correspondence:

Dr Nathalie Vergnolle,
Institut de Recherche en Santé Digestive (IRSD)
INSERM UMR-1220
Purpan Hospital, CS60039,
31024 Toulouse cedex 03 France
Phone : +33 5 62 74 45 00
E-mail : nathalie.vergnolle@inserm.fr

Word count: 4674

Data availability statement

The data supporting the findings of this study are available upon request from the corresponding author.

Funding statement

The doctoral salary of S.G was supported by Medical Research Foundation to NV (FRM - FDT202204014931) and National Research Institute for agriculture, feed and environment (INRAE) to CB. This study was supported by Paul Sabatier University, a grant of the European Research Council (ERC- 310973 PIPE) to NV, the ANR project TITAN (ANR-18-CE18-0019), the ANR project PARCURE (ANR-20-CE18-0024) and a grant from the Canadian Institutes of Health Research (CIHR) to MDH.

Author contribution statement

S.G., M.Sai., K.M., M.M., S.K., L.G., M.SeB., C.R. and M.A. performed experiments and analyses of the data. C.B., N.V. and M.D.H. contributed to the overall design of this study and data analysis. C.B., S.G., M.D.H., N.V., C.D., M.SeB., and M. Sav. contributed to the discussion and experimental design. L.B, E.B., B.B., L.A., C.C., C.D. and N.V. contributed to the acquisition of human material. C.B. and S.G. wrote the manuscript. All authors revised the manuscript.

Acknowledgments

Acknowledgements are due to the members of the animal housing facilities US006 (Toulouse): M. Lulka, T. Bernal, and R. Balouzat. We are grateful to Fabrice Pierre from UMR1331 Toxalim INRAE for providing CMT93 cells. The authors also acknowledge the U1220-IRSD Organoids Core facility for assistance in the collection of human mucus samples. We are grateful to members of NV-CD team for help and discussions.

Conflict of interest disclosure

The authors declare they have no actual or potential competing financial interests related to the work presented here.

Bullet point summary

What is already known?

- Chymotrypsin is a pancreatic serine protease of which the primary function is to break down food proteins in the gut lumen.
- PAR1 and PAR2 are protease-activated receptors expressed by intestinal epithelial cells at the apical and basal surfaces.

What this study adds

- Chymotrypsin is present and active in the close vicinity of the colonic epithelium and signals to epithelial cells.
- Chymotrypsin activates calcium and ERK1/2 signals downstream of PAR2 and disarms PAR1 from further activation by thrombin in intestinal epithelial cells.

Clinical significance

- The discovery of this novel signaling function for chymotrypsin opens new therapeutic avenues for pathologies involving PAR1 and PAR2.
- The very efficient PAR1 disarming effect of chymotrypsin could have a major clinical impact in the control of platelet activation.

Abstract

Background and purpose

Chymotrypsin is a serine protease produced by the pancreas and secreted into the lumen of the small intestine, where it digests food proteins. Due to its presence in the gut lumen, we hypothesized that chymotrypsin activity may be found close to epithelial cells and signals to them *via* Protease-activated receptors (PARs). We deciphered molecular pharmacology mechanisms for chymotrypsin signaling in intestinal epithelial cells.

Experimental approaches

The presence and activity of chymotrypsin were evaluated by western blot (WB) and enzymatic activity tests in luminal and mucosal compartments of murine and human gut samples. The ability of chymotrypsin to cleave the extracellular domain of PAR1 or PAR2 was assessed using cell lines expressing N-terminally-tagged receptors. The cleavage site of chymotrypsin on PAR1 and PAR2 was determined by HPLC-MS analysis. To study the pharmacology of chymotrypsin signals, we investigated calcium signaling and ERK1/2 activation using calcium mobilization assays and WB in CMT93 intestinal epithelial cells.

Key results

We found that chymotrypsin was present and active in the vicinity of the murine and human colonic epithelium. Molecular pharmacology studies evidenced that chymotrypsin cleaved both PARs receptors. While chymotrypsin activated calcium and ERK1/2 signaling pathways through PAR2, it disarmed PAR1, preventing further activation by its canonical agonist thrombin.

CONCLUSION

Our work suggests that the function of chymotrypsin in the gut lumen goes well beyond a simple digestive role. Our results highlight the ability of chymotrypsin to signal to intestinal epithelial cells *via* PARs, which may have important physiological consequences in gut homeostasis.

Keywords: chymotrypsin, intestinal epithelium, PAR1, PAR2, calcium signaling, MAPK, disarming cleavage.

INTRODUCTION

The intestinal epithelium is constantly exposed to luminal material such as microbiota, its metabolites, diet residues and host secretion products, including the pancreatic juice. The latter component contains a large amount of proteases (trypsins, chymotrypsins and elastases) that have an essential role in the digestion of dietary proteins (Pandol 2010). Although historically considered only as degradative enzymes, proteases are now viewed as true signaling mediators thanks to their ability to interact with PARs (Protease-Activated Receptors). PARs are GPCRs whose activation regulates many physiological and pathophysiological processes particularly in the gut (Adams et al. 2011; Vergnolle 2005, 2016; Sebert et al. 2019; Peach et al. 2023; Caminero et al. 2019; Alexander et al. 2021)

Unlike other GPCRs, the ligands for PARs are located within the extracellular N-terminus of the receptors themselves and are hence called tethered ligands (TL). The proteolytic cleavage of PARs at defined canonical sites situated at the N-terminal side of the TL enables its binding to the second extracellular loop of the cleaved receptor (Ramachandran et al. 2012). This binding induces conformational changes in the receptor that trigger downstream intracellular signals. However, while some proteases activate PARs by this mechanism, others have the ability to hinder PAR activation by cleaving their extracellular part at sites located downstream of the TL. This disarming cleavage makes them unusable for further proteolytic activation (Mihara et al. 2013; Dulong et al. 2003; Holzhausen et al. 2006). Nevertheless, some cleavages that sever the TL sequence downstream from the receptor's canonical activation site can also cause distinct signaling, a phenomenon called biased signaling (Ramachandran et al. 2011; Hollenberg et al. 2014). Synthetic agonist peptides mimicking the TL can also directly activate either uncleaved or N-terminally cleaved receptors, representing useful tools to study the pharmacology of PARs. Once activated, PARs can mediate a broad diversity of intracellular signals depending on the TL sequence unmasked by the cleaving protease and the ability of the receptor to interact with distinct G α protein subtypes (Ramachandran et al. 2012). Depending on the G α protein(s) involved, distinct signaling pathways have been described downstream of PAR activation

like Ca²⁺ mobilization, Mitogen-activated protein kinases (MAPK) phosphorylation, cAMP inhibition or Rho-associated kinase activation (Adams et al. 2011; Ramachandran et al. 2016; Ramachandran et al. 2012).

Four versions of PARs (PAR1-4) have been described, which are widely expressed throughout the body. Literature reports that PAR1 and PAR2 are the two main PARs expressed by the gut epithelium. PAR2 is strongly detected in the GI tract of humans and rodents, including in the stomach, the small intestine and the colon (Nystedt et al. 1994; Nystedt, Emilsson, et al. 1995; Nystedt, Larsson, et al. 1995; Bohm et al. 1996; Kong et al. 1997). Among the numerous cell types expressing this receptor, a clear immunolabelling of the epithelial compartment was reported in human and murine colon samples, especially at the apical side (D'Andrea et al. 1998; Cenac et al. 2002; Cuffe et al. 2002; Nasri et al. 2016). Lau and colleagues reported the existence of distinct apical and basolateral membrane pools of PAR2 in Caco2-BBe cells and in the mouse ileum (Lau et al. 2011). Regarding PAR1, while Darmoul and colleagues first indicated that this receptor is rather confined to cancerous colonic tissues and tumor-derived cell lines (Darmoul et al. 2003), many other publications suggest an expression of functional PAR1 in non-transformed intestinal epithelial cells (IECs) (Reinhardt et al. 2012; Sebert et al. 2018; Buresi et al. 2001). Activation of PAR1 by thrombin, its canonical protease agonist, promotes chloride secretion in non-transformed SCBN epithelial cells (Buresi et al. 2001). Moreover, apical stimulation of these cells with PAR1 agonists has also been reported to promote apoptosis (Chin et al. 2003), showing a functional PAR1 pool at membranes facing the lumen. Finally, both PAR1 and PAR2 have been shown to induce effects *in vivo* when their agonists are administrated intrarectally, likely involving direct activation of apical pools of receptors (Chin et al. 2003; Cenac et al. 2002; Motta, Palese, et al. 2021; Nguyen et al. 2003).

Chymotrypsin is a major serine protease produced by the pancreas and secreted into the gut lumen. Its primary and essential function is to digest dietary proteins into small peptides that can next be absorbed throughout the body. It is well established that pancreatic chymotrypsin is activated in

the duodenum, the intestinal segment where its proteolytic activity is highest (Borgstrom et al. 1957; Goldberg, Campbell, and Roy 1969). Chymotrypsin activity then progressively decrease along the small intestine, but is still elevated in the ileum. Of importance, active chymotrypsin has been detected at the surface of the small intestinal mucosa, highlighting a direct contact between this enzyme and the epithelial cells (Goldberg, Campbell, and Roy 1968). In addition, chymotrypsin activity is still detectable in human feces and was proposed as a marker for pancreatic exocrine function (Smith et al. 1971; Remtulla, Durie, and Goldberg 1986). Due to the presence of a thick mucus layer in the large intestine, whether chymotrypsin activity might be found at the vicinity of the colonic epithelium is still an open question. As well, its action on PARs and its potential effects on the host intestinal epithelium have never been addressed before.

In this study, we report the presence of active chymotrypsin neighboring the colonic mucosal surface. In addition, we identified that chymotrypsin is able to cleave PAR2 and activate downstream calcium and ERK1/2 signaling pathways in CMT93 colonic epithelial cells. Conversely, our results show that chymotrypsin disarms PAR1, hereby preventing further activation of the receptor by its canonical agonist thrombin. These results shed new light on the function of chymotrypsin in the gut, being able to regulate PAR-dependent signaling pathways.

MATERIAL AND METHODS

Reagents

All reagents were prepared according to the recommendations of the manufacturer. Chymotrypsin purified from bovine pancreas and treated with N α -Tosyl-L-lysine chloromethyl ketone hydrochloride (TLCK, a trypsin inhibitor) was prepared as stock solution at 1000 U/mL in 1mM HCl – 2mM CaCl₂ (Sigma-Aldrich, C3142). For some experiments, inactivated-chymotrypsin was prepared by heating for 1 hour at 95°C. Trypsin purified from bovine pancreas and devoid of chymotrypsin activity by TPCK treatment (Tosyl phenylalanyl chloromethyl ketone) (T1426), human plasma thrombin (T6884), the chymotrypsin inhibitor chymostatin (C7268), the cysteine protease inhibitor E-64 (E3132), the trypsin-like inhibitor TLCK (T7254), the aspartic protease inhibitor pepstatin A (P5318) and the serine protease inhibitor AEBSF (A8456) were all purchased from Sigma-Aldrich. The elastase inhibitor Elastatinal (sc-201272) was from Santa Cruz Biotechnology. The fluorogenic chymotrypsin substrate, Suc-Ala-Ala-Pro-Phe-AMC (aminomethyl coumarin) was provided by Bachem (4012873).

The C-terminally amidated PAR1 agonist peptide TFLLR-NH₂ and PAR2 agonist peptide SLIGRL-NH₂ were ordered from the GenScript company (20354 and RP19975 respectively). The PAR2 agonist peptide, 2-furoyl-LIGRLO-NH₂ (2fLI) and the PAR1 and PAR2 N-terminal peptides used for chymotryptic cleavage experiments (NATLDPRSFLLRNPNDKYE-NH₂ and TNRSSKGRSLIGKVDGTSHVTGKGVT-NH₂, respectively) were prepared by the peptide synthesis facility of the University of Calgary, Canada (>95% purity by HPLC). The PAR1 antagonist, F16357, was from Pierre Fabre Medicaments (Toulouse, France). The PAR2 antagonist I-191 was purchased from Axon Medchem (3043). BAPTA-AM (1,2-Bis(2-aminophenoxy)ethane-N,N,N',N'-tetraacetic acid tetrakis(acetoxymethyl ester)), a Calcium chelator was purchased at AbCam (ab120503). BTP2 (N-{4-[3,5-bis(Trifluoromethyl)-1H-pyrazol-1-yl]phenyl}-4-methyl-1,2,3-thiadiazole-5-carboxamide) was from Merck Millipore (203890), EGTA (ethylene glycol-bis(β -aminoethyl ether)-N,N,N',N'-tetraacetic acid) was purchased at Sigma-Aldrich (E3889). The following antagonists were used for signaling experiments: YM-254890 (G α q antagonist, AdipoGen

Life Sciences, AG-CN2-0509), Pertussis toxin (PTX) (G α i antagonist, Sigma-Aldrich, 516560) and Y-27632 (Rho-dependent G α 12/13 antagonist, Sigma-Aldrich, Y0503).

Human samples

All human biological samples were obtained from informed consenting patients treated at Toulouse Hospital (Centre Hospitalier Universitaire de Toulouse) after receiving ethics committee approval under protocol numbers CAPITOL RC31/21/038, COLIC DC-2015-2443, NCT05251415 and BACAP NCT02818829 (Canivet et al. 2018) approved by the relevant Comité de Protection des Personnes (CPP Sud-Ouest et Outre-Mer I et II).

Human colonic mucus was obtained from macroscopically healthy zones, taken during surgical resections in patients with colorectal cancer or inflammatory bowel diseases. Upon reception, tissues were mechanically cleaned of any residual fecal material and the surface of the mucosa was gently scraped using a cell scraper to harvest the mucus. The viscous material obtained was homogenized for 30 seconds using a Benchmark D1000 homogenizer, in a buffer containing 100 mM Tris-HCl pH8, 1 mM CaCl₂, 1mM CHAPS. The obtained mucus extract was then clarified by centrifugation (10 min – 2300 g at 4°C) and tested for the presence of chymotrypsin by proteolytic assays and Western-blot (WB) analyses.

Human colonic mucosal biopsies were obtained during colonoscopies in patients undergoing colorectal cancer screening. The tissue was placed in 300 μ L of the buffer described above and homogenized in tubes containing ceramic beads (6913500, MP Biomedicals) using a 3D bead-beating tissue homogenizer (Precellys, Bertin technologies) for 20 seconds at 6800 RPM and then centrifuged for 10 min at 2300 g. The obtained extract was then evaluated in WB to assess the presence of chymotrypsin.

Human stools were obtained from healthy donors and, upon receipt, divided into 2 differentially processed portions. Regarding batches dedicated to WB analysis, 30 mg were placed in 1.5 mL of Phosphate-Buffered Saline (PBS) supplemented with 0.01 % NP-40 lysis buffer, 0.1 % sodium

dodecyl sulfate (SDS), 12 mM deoxycholic acid and a protease inhibitor cocktail (Roche, 11836170001), then homogenized in tubes containing ceramic beads using a 3D bead-beating tissue homogenizer for 2x30 seconds at 5000 RPM and then centrifuged for 10 min at 1000 g. The resulting supernatants were mixed with Laemmli buffer (62.5 mM Tris-HCl pH6.8, 2 % SDS, 10 % glycerol, 0,01 mg/ml bromophenol blue, 5 % β -mercaptoethanol) after protein quantification by the BCA (Bicinchoninic acid Assay) method. For the assay of proteolytic activity, 30 mg of fecal samples were also placed in tubes containing ceramic beads and 1.5 ml of protease activity assay buffer (100 mM Tris-HCl pH8, 1 mM CaCl_2 , 1 mM CHAPS). Samples were then homogenized for 2x30 seconds at 5000 RPM with a Precellys tissue homogenizer, and finally clarified by centrifugation (10 min – 2300 g at 4°C).

Human pancreatic tissue was obtained from a surgical resection during Whipple procedure. The tissue was homogenized in TRI Reagent® (TR 118, Molecular Research Center) using a Benchmark D1000 homogenizer. After addition of 200 μL chloroform, centrifugation at 12000 g for 15 min at 4°C and removal of the aqueous phase, protein precipitation was performed on the remaining organic phase by mixing it with 1 volume of isopropanol. After centrifugation at 2000 g for 20 min at 4°C, the protein pellet was washed twice with 50 % ethanol and resuspended in 2% SDS.

Mouse samples

All animal experiments were conducted in compliance with the European legislation on animal research and with ARRIVE 2.0 guidelines. C57BL/6J mice were used in this study. They were initially purchased from Janvier Laboratory (France) and bred at the US006/INSERM animal facility (Toulouse) in ventilated cages (5 mice maximum/cage) in a specific pathogen-free area. They had free access to food and water and were maintained in a 12-hour light/dark cycles. They were moved and acclimated to the local animal facility at least 1 week before sacrifice at 7 to 12 weeks of age. This was done by cervical dislocation after collection of fresh feces which were immediately frozen in liquid nitrogen. From these fecal samples, native protein extracts were prepared as follows and used for WB and proteolytic assay. Frozen murine stools were homogenized twice in 1.5 mL of RIPA buffer (1% NP40,

0,5% deoxycholic acid, 0,1% SDS) during 30 seconds at 4500 RPM using a Precellys tissue homogenizer followed by removal of insoluble material by a 10-min centrifugation at 2300 g and 4°C.

Murine pancreas was resected and prepared as described for human pancreas. Lung protein extracts were prepared by homogenization in lysis buffer (Pierce IP Lysis Buffer, ThermoFisher Scientific) using the 3D bead-beating tissue homogenizer for 2x30s at 6800 RPM, followed by removal of solid residual material by centrifugation at 13000 g for 5 min at 4°C.

The colon was resected and mucosal scrapings were performed using different strategies. In order to preserve the mucosa-associated material for proteolytic activity and WB assays, the colon was opened longitudinally, the residual fecal material was mechanically removed and mucosa was scraped using a microscopy slide. In contrast, for some WB experiments, the luminal surface of the colon was previously washed with 15 mL of PBS before opening, in order to remove any mucosa-associated material and retain only the host mucosal cells. This washed mucosa was then scraped as described above. All mucosal scrapings were then homogenized for 2x15 seconds at 4500 RPM using a Precellys tissue homogenizer in lysis buffer supplemented with a cocktail of protease inhibitors (100 µM E-64, 100 µM pepstatin, 135 µM TLCK and 100 µM elastatinal) targeting a wide spectrum of protease activities except those belonging to the chymotrypsin family. All samples were then cleared of residual solid particles by centrifugation (13000 g – 5 min – 4°C) before analyses.

Preparation of PAR2-null HEK293 and CMT93 cells

PAR2^{-/-} Human Embryonic Kidney cells (HEK293) were derived from the HEK293 cell line constitutively expressing functional PAR1 and PAR2 (Kawabata et al. 1999), using a CRISPR approach similar to that described for the generation of PAR1^{-/-} HEK293 cells in Mihara *et al.* (Mihara et al. 2016). The three target sequences for CRISPR knockout of PAR2 were derived from the human PAR2/F2RL1 genomic sequence. [HGLibA_15864: GTCTGCTTCACGACATACAA, HGLibA_15865: GGAACCAGTAGATCCTCTAA, HGLibA_15866: CCCAGCAGCCACGCCGCGC]. Cells were transfected with

Lipofectamine LTX (ThermoFisher Scientific) and maintained in the presence of 5 $\mu\text{g}/\text{ml}$ puromycin to select knockout cells.

Murine colonic epithelial CMT93 cells deficient for PAR2 (PAR2^{-/-}) were generated using Crispr/Cas9 technology as described in Nasri *et al.* (Nasri *et al.* 2016). Briefly, CMT93 cells were electroporated with mPAR2 Crispr/Cas9 plasmid (sc420265, Santa Cruz Biotechnology). Transfected cells were sorted by flow cytometry to isolate GFP-positive cells from which clones were isolated and amplified.

Both HEK and CMT93 PAR2^{-/-} cells were validated by checking loss of calcium mobilization effect in an assay using PAR2 agonist peptides (Supp. Figure S1A, B).

Cloning and transfection of CHO cells

Engineered receptors with a nanoLuciferase (nLuc) inserted at the N-terminus of human PAR1 or PAR2 were created to monitor the extracellular cleavage of PAR molecules. These receptors also contained an eYFP inserted at the C-terminus of PAR1 or PAR2. The details of the construction strategy are as follows.

The pCDNA3.1-hPAR1 and pCDNA3.1-hPAR2 were obtained from cDNA Recourse Center (Bloomsburg, PA). The nLuc containing vector (pNL1.1) was a gift from Promega (Madison WI). The stop codon of hPAR1 in pCDNA3.1 was replaced by a tyrosine-encoding codon by site-directed mutagenesis and the coding sequence of eYFP (flanked by XhoI and XbaI restriction sites) was cloned downstream and in frame of the PAR1 sequence, giving a pCDNA- PAR1-eYFP vector. Restriction sites of BspEI and BamHI were then added by site directed mutagenesis at S31 of PAR1 allowing insertion of a nanoLuciferase PCR fragment upstream of the PAR1-eYFP cDNA. The resulting vector was named pCDNA-nLuc-PAR1-eYFP. For PAR2, similar constructs were generated using this strategy (nLuc inserted at Q27 site of hPAR2). CHO-K1 cells were transfected with the nLuc-hPAR1/2-eYFP pCDNA plasmids using the GeneJuice[®] transfection reagent kit (Sigma-Aldrich, 70967), according to the manufacturer's

instructions. The transfected cells were selected with G418 at 1.5 mg/ml (Sigma-Aldrich, A1720) during one week.

For other experiments, site-directed mutagenesis was performed on the pcDNA3.1-hPAR2 to create a R³⁶/G mutant of hPAR2, using the QuikChange Lightning Multi Site-directed Mutagenesis Kit (Agilent Technologies, Mississauga, ON). This plasmid was transfected in double deficient PAR1^{-/-} and PAR2^{-/-} HEK cells.

Cell culture

All cell lines were maintained at 37°C and 5% CO₂ and medium was changed every two days. Cells were subcultured when they reached 90% confluence.

CMT93 cells (ATCC-CCL-223) were grown in Dulbecco's modified eagle's medium (DMEM, Gibco) supplemented with 100 U/ml penicillin/streptomycin, 10% fetal calf serum (FCS) and 1% Non-Essential Amino Acids Solution (NEAA). PAR2^{-/-} CMT93 cells were grown in a similar medium supplemented with G418 0.7 mg/mL.

CHO cells stably transfected with nLuc-PAR1/2-YFP were cultured in Ham-F12 (Gibco) supplemented with 10% FCS, 1% NEAA, in the presence of G418 at 0.7 mg/mL.

All HEK293 cells (wild-type (WT) and mutant), were routinely maintained in DMEM supplemented with 1 mM sodium pyruvate, 10% FCS, and 2.5 µg/ml of plasmocin (InvivoGen, San Diego, CA). Sub-culturing was performed without trypsin by cell dissociation using enzyme-free buffer (PBS pH7.4, containing 1 mM EDTA). The CRISPR-derived PAR2^{-/-} HEK cells were maintained in regular medium containing 5 µg/ml puromycin to preserve their knockout status.

Determination of PAR1 and PAR2 cleavage sites by chymotrypsin

Peptides corresponding to a region of the N-terminal extracellular domain of human PAR1 and PAR2 containing the TL sequence were produced at the Faculty of Peptide Synthesis at the University of Calgary. hPAR1: NATLDPRSFLLRNPNDKYE; hPAR2: N-acetyl-GTNRSSKGRSLIGKVDGTSHVTGKGVT-

amide; (TL activating sequences are underlined). Peptides (100 μ M final) were incubated with chymotrypsin 5 U/ml for 30 min at 37 °C. Reactions were stopped by adding 1 volume of 50% acetonitrile and 0.1% trifluoroacetic acid in water. Samples were fractionated by reverse-phase HPLC, and eluted peptides were analysed by mass spectrometry as outlined previously (Oikonomopoulou et al. 2006).

Detection of ERK1/2 activation

WT or PAR2^{-/-} CMT93 cells were plated at 250 000 cells/well in 6-well plates in culture medium. The day after, cells were washed three times in PBS and maintained in Hank's Balanced Salt Solution (HBSS, Gibco, 14025092) for 16h. Cells were then stimulated with different concentrations of chymotrypsin for 10 minutes. At the end of incubation, cells were placed on ice, washed once in PBS and lysed in the IP Lysis Buffer (ThermoFisher Scientific) supplemented with protease inhibitor (cOmplete™, Roche) and phosphatase inhibitor cocktail (P5726, Sigma-Aldrich). Some experiments were performed in the presence of antagonists: cells were incubated for 16h with PTX (100 ng/mL), 10 minutes with Y-27632 (10 μ M) or 5 minutes with YM-254890 (10 μ M) before stimulation by chymotrypsin. Protein lysates were centrifuged at 1000 g for 5 minutes at 4°C to eliminate insoluble material. These extracts were diluted in LDS NuPAGE buffer (Invitrogen) supplemented with 5% β -mercaptoethanol and used for WB analysis.

Equal amounts of total proteins (5 μ g, according to BCA protein assay) were separated by SDS-PAGE on 4-15% Mini-PROTEAN® TGX™ precast gels (Bio-rad) and transferred to nitrocellulose membranes. After blocking in PBS containing 0.2 % Tween 20 and 5 % milk, p42/p44 MAPK phosphorylation was detected using anti-phospho p42/p44 rabbit monoclonal IgG (Cell Signaling Technology, #4370) diluted 1/2000 in blocking buffer and incubated overnight at 4°C. Bound anti-phospho p42/p44 were probed with HRP-conjugated anti-rabbit antibodies (Promega, W401B) diluted 1/3000 in blocking buffer. Peroxidase activity was visualized upon addition of ECL western blotting reagents (GE Healthcare) using a ChemiDoc MP Imaging System (Bio-Rad). The membranes were

stripped during 20 minutes using a buffer containing 1% SDS, 0.1% Tween 20, 15 g/L glycine and 0.37% HCl, washed with PBS-Tween 0.2% and incubated in blocking buffer for 1h. The absence of residual signal was systematically verified by ECL revelation. To normalize the phosphorylated p42/44 signals, the membranes were probed overnight at 4°C with a rabbit anti-p42/44 antibody recognizing both phosphorylated and unphosphorylated forms (Cell Signaling Technology, #9102) detected as described above. Image Lab software 6.1 (Bio-Rad) was used to quantify the densitometric analyses of the p42/44 signals.

Detection of chymotrypsin in human and mouse samples by Western Blot

For the following WB experiments, different amounts of protein extracts from murine and human gut samples (see below) were loaded to adapt to different chymotrypsin abundance among the samples and to avoid signal saturation. The amount of loaded proteins prepared in laemmli were as follows: 2 µg and 0.1 µg for human and murine pancreas, respectively; 25 µg and 17 µg for human and mouse feces, respectively; 40 µg, 50 µg and 7 µg for murine colonic scrapings, human mucus and human colonic biopsy, respectively. Protein extracts were then resolved on 4-15% gradient acrylamide gels as described in the previous section. Migration, transfer, blocking, ECL detection, steps were carried out as described above. We systematically performed a first incubation with secondary antibody alone in order to verify the absence of cross-reactivity of this antibody. After this validation, the membranes were incubated with the primary antibody followed by the secondary antibody. To avoid nonspecific binding, different antibodies were used for human and murine samples. For human samples, the primary antibody was an anti-CTRB1/2 mouse monoclonal IgG (D-5, Santa Cruz, sc-393414) and the secondary antibody was an HRP-coupled goat anti-mouse IgG (Jackson ImmunoResearch, 115-035-166). For murine samples, we used an anti-CTRB1/2 goat monoclonal IgG (F-13, Santa-Cruz, sc-161496) followed by an HRP-coupled donkey anti-goat IgG (Promega, V8051).

Assay of chymotryptic proteolytic activity

The specific chymotrypsin activity was measured in murine stool and colonic scraping extracts by following the degradation of the chymotrypsin peptide substrate, Suc-Ala-Ala-Pro-Phe-aminomethyl coumarin (AMC). 50 μ L of extracts were placed in a 96 well plates and pre-incubated for 20 min at 37°C. The enzymatic reaction was started by adding an equal volume of 1 mM substrate solution (diluted in 100 mM Tris-HCl pH8, 1 mM CaCl₂) to the samples. Substrate cleavage, leading to free AMC release, was monitored by measuring fluorescence (excitation: 360 nm, emission: 460 nm) every 30 seconds during 20 minutes in a Varioskan Flash microplate reader (ThermoFisher Scientific). The initial velocities of the curves were extracted from the kinetic graphs using the SkanIt™ software (ThermoFisher Scientific). The presence of a specific chymotrypsin-like activity in the samples was confirmed by comparison with the values obtained in the presence of the selective inhibitor chymostatin (500 μ M). The proteolytic activity was quantified in U/mL using a standard curve generated with increasing concentrations of commercial pancreatic chymotrypsin. Proteolytic activity was normalized to protein content measured with a BCA protein assay.

The same protocol was used to measure proteolytic activity in human stool and mucus extracts except that 1mM CHAPS detergent was added to buffer for the dilution of the extracts, substrates and commercial chymotrypsin.

Luciferase assay for measuring release of N-terminally tagged PARs

The ability of chymotrypsin to cleave and release the N-terminal domain of PAR1 and PAR2 was assessed essentially as described previously (Mihara et al. 2016), using CHO cells stably expressing hPAR1 or hPAR2 with a luciferase tag on the N-terminal extremity and luciferase activity was monitored in the cell medium, as follows. CHO-nLuc-PAR1 or PAR2 were plated in 96 well plate at 20 000 cells/well and cultured for 48h. The cells were then washed 3 times with HBSS and incubated with increasing concentrations of chymotrypsin during 10 minutes at 37°C. After exposure to chymotrypsin, cell supernatants potentially containing the cleaved PAR N-terminus (with nLuc tag) were collected and proteolytic activity was stopped by adding 1 mM of the broad-spectrum serine inhibitor AEBSF.

Any contaminating cell debris was removed by centrifugation 5 min – 160 g. Using a Varioskan plate reader, luciferase activity was assayed in 50 μ L of cell supernatant by recording luminescence during 5 minutes in white 96 well plates, after addition of 50 μ L of the luciferase substrate provided in a Luciferase assay kit (Nano-Glo[®] Luciferase Assay System, N1110, Promega). Luciferase signals were proportional to the amount of PAR cleaved on the cell surface. Luciferase release by chymotrypsin was normalized to the total bioluminescence yielded by untreated cells.

Calcium mobilization assay

CMT93 cells (WT or PAR2^{-/-}) were plated at 20 000 cells/well in black clear-bottomed 96-well plates (Greiner Bio-One, 655090) and grown for 48 hours. Cells were washed 2 times in HBSS (Gibco, 14025092) and incubated for 1h at 37°C with 100 μ L of Fluo8 calcium probe (Screen Quest[™] Fluo8 calcium AAT bioquest[®]) prepared following the manufacturer recommendations. After one wash in HBSS, 100 μ L of HBSS was added and the cells were stimulated at 37°C while simultaneously monitoring calcium signals using an injector-equipped microplate reader (NOVOstar, BMG Labtech). For all the experiments performed in the absence of extracellular calcium, Ca²⁺-free HBSS (Gibco, 14175095) supplemented with 20 μ M EGTA was used during cell stimulations. The recording of the calcium response started 4 sec before cell stimulation (corresponding to the baseline values) and lasted up to 200 seconds. Curves were normalized by dividing each value by the baseline value so each graph is starting at 1. In some experiments, cells were stimulated twice.

For some experiments, antagonists were added before stimulation with chymotrypsin and were continually present until the end of the experiment. For G α antagonists, cells were incubated for 16h with PTX (100 ng/mL), 10 minutes with Y-27632 (10 μ M) or 5 minutes with YM-254890 (10 μ M). The intracellular calcium chelator BAPTA-AM was used at 30 μ M and incubated for 1h with cells prior stimulation with chymotrypsin, its vehicle was 0.03% DMSO. To determine the involvement of CRAC in the calcium response, cells were first incubated during 30 minutes with 10 μ M of the CRAC channel antagonist, BTP2 (vehicle: 0.04% DMSO). Cells were then stimulated with chymotrypsin in calcium-free

HBSS. Recording was done every 2s and an injection of CaCl₂ solution was done 4 minutes after the chymotrypsin treatment in order to reach 2 mM calcium concentration, enabling calcium influx from the medium to the cell cytoplasm. The magnitude of this calcium influx was quantified by calculating Area Under the Curves (AUC).

For HEK cells, measurements of calcium signaling induced by synthetic agonist peptides were conducted essentially as described previously (Mihara *et al.* 2016 ; Kawabata *et al.* 1999). Briefly, cells were lifted from a culture flask with EDTA-supplemented calcium-free isotonic phosphate-buffered saline (pH 7.4), washed, and resuspended at approximately 5.10⁷ cells/ml in HBSS supplemented with 10mM HEPES, 1.5mM CaCl₂, and 1.5mM MgCl₂ containing Fluo4 calcium indicator (ThermoFisher Scientific). Agonists were added to 2 mL-stirred cell suspensions in a spectrofluorometer (Perkin-Elmer), and the fluorescence emission signal at 530 nm (excitation wavelength, 480 nm) was measured to follow the intracellular calcium response.

Statistical analyses

All graphical figures and statistical analyses were performed with the GraphPad Prism 9.4.1 software (GraphPad Software, San Diego, California USA). For single comparisons, statistical differences were assessed with the nonparametric Wilcoxon matched-pairs signed-rank test. For multiple comparisons, the Friedman test was used, followed by the Dunn's test for multiple comparisons. For disarming experiments, different concentrations of chymotrypsin were tested independently for technical reasons, thus a Kruskal-Wallis test was employed followed by the Dunn's post-test. In all cases the significance level was fixed at p<0.05. Regarding PAR1 and PAR2 cleavage experiments and PAR1 disarming, concentration–response curves were fitted in GraphPAD with log-transformation of the chymotrypsin concentrations followed by a non-linear regression for normalized responses with a standard Hill slope of 1 (agonist) or -1 (inhibition).

RESULTS

The epithelium is exposed to chymotrypsin activity throughout the intestinal tract

Chymotrypsin has been shown to adsorb easily to the surface of small intestinal epithelial cells without loss of activity (Goldberg, Campbell, and Roy 1968). However, such proximity has never been addressed in the colon where the epithelium is covered by a thick mucus layer. In this context, we first explored the presence of chymotrypsin in protein extracts of different mouse and human colonic compartments by WB analyses. We used antibodies directed against the major pancreatic chymotrypsin form, chymotrypsin B (CTRB). As shown in Figure 1A, in murine pancreatic extracts, we confirmed the presence of a unique signal at 26-kDa that corresponds to the molecular weight of CTRB. As expected, no such signal was detected in lung, since this organ does not express CTRB. In colonic compartments, we found that CTRB signal was immunodetected in stools as well as in colonic mucosal scrapings, but only when the mucosa-associated material, including the mucus layer, were preserved (unwashed). The CTRB signal was indeed not observed in mucosal scrapings realized after extensive elimination of the luminal material. This result shows that the colonic mucosa is not an endogenous producer of CTRB and that this enzyme does not penetrate the epithelium. Similar results were found in human samples, where a specific CTRB signal was clearly visible not only in stools but also in colonic mucus, whereas the human colonic mucosa was negative for CTRB (Figure 1A). These results highly suggest that in physiological conditions, chymotrypsin infiltrates the mucus layer and may reach the surface of the mouse and human colonic epithelium.

To assess whether chymotrypsin protein detected in the different gut compartments was active, we measured chymotrypsin proteolytic activity by enzymatic assay (Figure 1B). Using Suc-Ala-Ala-Pro-Phe-AMC substrate, we found that human and mouse stools contained a substrate-cleaving activity that was fully inhibited by chymostatin, a specific inhibitor of chymotrypsin-like activities. As well, chymotrypsin activity was also detected in unwashed mucosal scrapings from mouse and human mucus. Altogether, our data highlight the presence of active chymotrypsin in the vicinity of the colonic

epithelium, both in mouse and human. In addition to the small intestine, these findings support that an interaction between chymotrypsin and the surface of IECs might also occur in the distal segments of the GI tract.

Chymotrypsin cleaves PAR2 and activates calcium signaling in intestinal epithelial cells

Due to the presence of active chymotrypsin neighbouring the small intestinal and colonic mucosa, we investigated the possible regulation of Protease-activated Receptors (PARs) by chymotrypsin. We focused on PAR1 and PAR2 which are both expressed at the apical surface of IECs (Bohm et al. 1996; Kong et al. 1997; Cenac et al. 2002; Cuffe et al. 2002; Lau et al. 2011).

We first assessed the ability of chymotrypsin to cleave the extracellular domain of PAR2. To do so, CHO cells stably expressing PAR2 receptor fused to a nanoLuciferase tag on its N-terminal extremity were treated with active chymotrypsin. As shown in Figure 2A, incubation of chymotrypsin with the reporter cells led to the release of luciferase activity into the culture medium in a concentration-dependent manner. These data show that chymotrypsin is able to cleave within the N-terminal extremity of PAR2.

We next investigated the ability of chymotrypsin to induce calcium mobilization downstream of PAR2 cleavage in IECs. We used the CMT93 colonic epithelial cell line that endogenously expresses high levels of PAR2 (Nasri et al. 2016). As illustrated in Figure 2B, chymotrypsin was able to generate a concentration-dependent calcium signaling in WT CMT93 cells. This calcium response was completely abolished when PAR2-deficient (PAR2^{-/-}) cells were used. In addition, the use of a PAR2 antagonist (I-191 at 10 μM) drastically reduced the calcium response (Figure 2C). These experiments reveal that chymotrypsin drives calcium signaling in intestinal epithelial CMT93 cells exclusively *via* PAR2.

We then employed antagonists against the different Gα protein subunits known to be involved downstream PAR2 activation (YM-254890 for Gαq, Pertussis toxin (PTX) for Gαi or Y-27632 for Rho-

dependent $G\alpha_{12/13}$). Pre-treatment of cells by PTX or Y-27632 had no effect on the chymotrypsin-induced calcium response, whereas YM-254890 prevented it (Figure 3). This indicates that the calcium mobilization triggered by chymotrypsin *via* PAR2 is totally dependent on $G\alpha_q$ proteins. Together, our results show that chymotrypsin activity is able to cleave PAR2 and trigger a $G\alpha_q$ -dependent calcium signaling in IECs.

PAR2 activation by chymotrypsin mediates Store-operated calcium entry (SOCE) in CMT93 cells

Interestingly, the kinetics of the increase in intracellular calcium caused by chymotrypsin differed from the kinetics observed with the PAR2 canonical agonists trypsin or SLIGRL (compare Figure 2B and Supp. Figure S1B, C). These classical activators caused an early peak of intracellular calcium immediately followed by a decrease, without any increase afterwards. In contrast, with chymotrypsin, the first calcium peak was consistently followed by a sustained plateau or increasing phase of calcium signal.

Then, we analyzed in detail the chymotrypsin-induced calcium signal in the goal to determine the involvement of intracellular and/or extracellular calcium. The use of BAPTA-AM, a membrane permeant chelator, that traps the intracellular calcium prevented the signaling induced by chymotrypsin (Figure 4A), demonstrating that chymotrypsin-induced calcium signal is dependent on release from calcium intracellular stores. Then, the use of calcium-free medium during cell stimulation by chymotrypsin significantly lowered the plateau phase while maintaining the first peak of intracellular calcium (Figure 4B). These results strongly suggest that chymotrypsin induces a calcium response initiated by a release of calcium from intracellular stores followed by an influx of calcium from the extracellular medium.

We investigated the role of CRACs (Ca²⁺ Release-Activated Ca²⁺ Channels) in this pathway. Indeed, these proteins belong to a family of plasma membrane calcium channels named ORAI that are activated by intracellular store depletion *via* STIM sensors located in the endoplasmic reticulum membranes. The interaction between STIM and ORAI proteins triggers channel opening and subsequent entry of extracellular calcium into the cytosol, a process called Store-Operated Calcium Entry (SOCE) (Yoast, Emrich & Trebak, 2020). We found that all CRAC components: *Orai1*, *2* and *3* channels as well as *Stim1* and *Stim2* were expressed in CMT93 cells (Supp. Figure S2). Therefore, we investigated the role of CRACs in the delayed calcium response using a two-step strategy to uncouple the intracellular store mobilization from the extracellular influx of calcium. As shown in Figure 4C, CMT93 cells were first stimulated with chymotrypsin (arrow) in the absence of extracellular calcium. As expected in these conditions, the protease triggered a calcium mobilization from intracellular stores in cells (as previously observed in Figure 4B, calcium-free conditions). After return to a basal fluorescence signal, the addition of a Ca²⁺ solution (2 mM final) in the extracellular medium resulted in a substantial entry of calcium into the cells. This calcium influx was quantified by calculating AUC. Pre-treatment of cells with the CRACs antagonist BTP2 significantly reduced the amplitude of calcium influx, showing that chymotrypsin triggered CRAC activation downstream PAR2 in CMT93 cells.

Altogether, our results showed the ability of chymotrypsin to cleave PAR2 and activate a Gαq-dependent increase in intracellular calcium which is composed of 2 phases: a first release from ER stores, followed by a CRAC-mediated Store-Operated Calcium Entry from the extracellular environment.

Chymotrypsin activates ERK1/2 signaling downstream of PAR2 in intestinal epithelial cells

In addition to calcium signaling, we also evaluated whether chymotrypsin could activate the ERK1/2 pathway *via* PAR2 in CMT93 cells. For this purpose, we stimulated WT or PAR2^{-/-} CMT93 cells for 10 minutes with different concentrations of chymotrypsin. The ratios between phosphorylated and

total ERK1/2 were quantified by WB in the protein extracts to evaluate the ERK1/2 activation levels. Figure 5A shows the ability of chymotrypsin to activate the ERK1/2 signaling pathway specifically via PAR2 in CMT93 cells, since the absence of this receptor (PAR2^{-/-}) significantly reduced the ERK1/2 phosphorylation levels. As a control, heat-inactivated chymotrypsin was not able to trigger ERK1/2 activation. Finally, pre-treatment of cells with PTX or YM-254890, but not with Y-27632, significantly reduced the PAR2-dependent ERK1/2 activation caused by chymotrypsin (Figure 5B).

Interestingly, in contrast to chymotrypsin, trypsin was still able to activate ERK1/2 pathway in the absence of PAR2 (Supp. Figure S3). Our data also showed that trypsin could trigger an elevation of intracellular calcium in PAR2^{-/-} CMT93 cells (Supp. Figure S1C). These results highlight functional differences between trypsin and chymotrypsin in terms of molecular targets at the cell surface.

Altogether, our data indicate that the cleavage of PAR2 by chymotrypsin induces ERK1/2 signaling pathway involving G α i and G α q proteins. In addition, in contrast to what was observed with trypsin, chymotrypsin-associated calcium and ERK1/2 signaling pathways are exclusively dependent on PAR2.

Chymotrypsin cleaves PAR2-derived synthetic peptides at a non-canonical site *in vitro* but might use the canonical site in a cellular context

To determine the cleavage sites of PAR2 by chymotrypsin, we performed *in vitro* digestion of a synthetic hPAR2 N-terminal peptide (GTNRSSKGR**SLIGKVD**GTSHVTGKGVT-NH₂) encompassing the canonical tethered ligand sequence (**SLIGKV**) and determined the sequence of the generated cleavage products by HPLC-MS analysis (Figure 6A). This peptide was incubated with 5 U/mL chymotrypsin for 30 minutes. The HPLC peak generated by chymotrypsin corresponded to a cleavage of the parental peptide 2 amino acids downstream of the trypsin canonical R³⁶/S³⁷ cleavage site, i.e. at L³⁸/I³⁹. This generated the **IGKVD**GTSHVTGKGVT-NH₂ C-terminal peptide which lacks S³⁷-L³⁸. Intriguingly, the

complementary N-terminal peptide (GTNRSSKGRSL) was not detected. We suspect that this peptide was rapidly digested by chymotrypsin during these experiments. The two amino acids S³⁷-L³⁸ were described as essential to generate a PAR2-dependent calcium signaling in HEK cells (Ramachandran et al. 2009). We therefore reasoned that the L³⁸/I³⁹ cleavage site, which removes S³⁷-L³⁸, was unlikely to generate the chymotrypsin induced-calcium response. We investigated this hypothesis using HEK cells, a human cell line widely used for the study of PAR pharmacology. We first validated that chymotrypsin was able to generate a calcium signal in WT HEK cells, with a plateau phase as observed in CMT93, which was totally abolished in PAR2^{-/-} cells (Figure 6B). We then constructed a mutant version of hPAR2 obtained after site-directed mutagenesis of wild-type hPAR2 sequence at the canonical site (R³⁶G). This construction was transfected in double PAR1 and PAR2 deficient HEK cells. In those transfected cells, no calcium signal was observed downstream stimulation by chymotrypsin or trypsin, while treatment with the PAR2 agonist peptide 2fLI was still able to trigger a calcium response, validating the functionality of the transfected PAR2 R³⁶G mutant receptors (Figure 6C). These data highly suggest that, in contrast to what happens in the *in vitro* cleavage assay, chymotrypsin is cleaving at the canonical site of PAR2 to induce calcium signaling *in cellulo*. In line with this idea, our data revealed that neither a short (IGKVDGT-NH₂) nor a long (IGKVDGTSHVTGKGVT-NH₂) synthetic peptide, corresponding to the sequence unmasked by the L³⁸/I³⁹ cleavage site, activated calcium or ERK1/2 signaling in HEK cells (Supp. Figure S4).

Overall, our data suggest that chymotryptic activity is able to cleave PAR2 at the R³⁶/S³⁷ and L³⁸/I³⁹ sites, but only the R³⁶/S³⁷ cleavage site appears to be responsible for the downstream activation of calcium and ERK1/2 signals in living cells.

Chymotrypsin disarms PAR1

Since PAR1 is also expressed in IECs, we next explored the possible action of chymotrypsin on this receptor. As done for PAR2, the cleavage of the N-terminal domain of PAR1 was investigated by

incubating CHO cells stably expressing nanoLuciferase-hPAR1 with increasing concentrations of chymotrypsin. As illustrated in Figure 7A, chymotrypsin was able to release N-terminal peptides containing luciferase from the tagged PAR1 in a concentration-dependent manner. The PAR1 cleavage site was then determined by *in vitro* digestion of a synthetic hPAR1 N-terminal peptide followed by HPLC-MS analysis. This experiment revealed a unique cleavage site localized within the canonical tethered ligand sequence, at F⁴³/L⁴⁴ (Figure 7B). To investigate the consequences of PAR1 cleavage by chymotrypsin, we took advantage of PAR1 expression and functionality in WT and PAR2^{-/-} CMT93 cells (Nasri et al. 2016). As inferred from our experiments in PAR2-deficient (but PAR1-expressing) CMT93 cells, the cleavage of PAR1 by chymotrypsin did not generate any signaling (Figure 2B and Figure 5A). According to these results, we hypothesized that the chymotrypsin-mediated cleavage of PAR1 within the tethered ligand sequence would disarm rather than activate the receptor.

We therefore investigated the possibility for chymotrypsin to impede further cleavage and signaling induced by thrombin, the canonical activator of PAR1, known to cleave at the R⁴¹/S⁴² site to unmask the tethered ligand SFLLR. In PAR2^{-/-} CMT93 we showed that the thrombin-induced calcium response is totally attributable to PAR1 since the use of the PAR1 antagonist F16357 totally abolished the calcium response (Figure 8A). In order to test the ability of chymotrypsin to prevent the PAR1-mediated calcium response induced by thrombin, we carried out sequential incubations with chymotrypsin and then thrombin (Figure 8B). To prevent the possible degradation of thrombin by chymotrypsin, chymotrypsin was removed before the addition of thrombin. Figure 8C illustrates the calcium response recorded during the second stimulation of CMT93 cells with thrombin (or HBSS). As a positive control, the pre-incubation of cells with thrombin fully prevented the calcium response induced by a second stimulation with thrombin, due to the desensitization of the receptor (Figure 8C-D). Similarly, the pre-incubation of cells with 10 U/mL chymotrypsin totally abolished the calcium response normally induced by thrombin. This disarming effect was concentration-dependent as illustrated in figure 8E-F, with an IC₅₀ of 0.02 U/mL. The functionality of PAR1 in cells pre-treated or not

with chymotrypsin remained intact since calcium responses upon addition of TFLLR, the PAR1 agonist peptide, were not significantly impacted (Figure 8G).

Taken together, our study shows that chymotrypsin does not activate PAR1, but instead, prevents thrombin-dependent signaling by cleaving PAR1 two amino acids downstream of the canonical cleavage site.

DISCUSSION

Our manuscript describes for the first time a signaling role for pancreatic chymotrypsin that we found present and active in the vicinity of the colonic epithelium. The potential intracellular signals resulting from the interaction between chymotrypsin and the intestinal epithelial cells had never been explored so far. Our study clearly demonstrates that PAR1 and PAR2, two GPCRs expressed at the surface of IECs, are cleaved by this digestive enzyme. While the cleavage of PAR2 by chymotrypsin is able to transduce important intracellular signalling pathways, PAR1 cleavage prevents further signaling in response to thrombin, its canonical agonist (general schematic representation in Figure 9).

In addition to the small intestine, our data show that the apical side of the colonic epithelium is neighbored by active chymotrypsin under physiological conditions. Nevertheless, we observed a high heterogeneity in chymotrypsin activity present in feces and mucus-containing extracts. This variability might be explained by the fact that pancreatic juice is not permanently secreted into the gut lumen, but regulated by food intake through humoral and neuronal controls (Singer and Niebergall-Roth 2009). A similar variation was also observed in another study analysing the chymotrypsin activity content in infant stools (Remtulla, Durie, and Goldberg 1986). Accordingly, the molecular pathways that we describe in this study involving chymotrypsin and its cleaving activity on PAR1/2 are likely to operate physiologically in the gut, but in a discontinuous manner.

Our results demonstrate that chymotrypsin activates intracellular calcium signaling and ERK1/2 pathways exclusively through PAR2 in the IEC cell line CMT93. Knowing that PAR2 has been shown to exert pleiotropic functions, one can predict an array of physiological consequences chymotrypsin could have on gut homeostasis. *In vivo*, the intraluminal administration of PAR2 activators has been observed to increase epithelial paracellular permeability (Roka et al. 2007; Cenac et al. 2002). In addition, publications have also reported that stimulation of PAR2 in IEC cell lines triggers electrolyte transport, chemokine or eicosanoid secretion and inhibition of cytokine-induced apoptosis (van der Merwe, Hollenberg, and MacNaughton 2008; Kong et al. 1997; Iablokov et al. 2014;

Tanaka et al. 2008). Regarding chymotrypsin, one study has revealed that this enzyme triggered a decrease of ion permeability in SCBN cells, which was dependant on PKC-zeta activation but not on PAR2 (Swystun et al. 2009). Functional studies will be needed in the future to address the role of the chymotrypsin-PAR2 axis in the context of gut epithelial cells.

From a mechanistic point of view, we found that chymotrypsin activated ERK1/2 pathway downstream PAR2, *via* G α i and G α q proteins. PAR2 activation by chymotrypsin also triggered calcium signaling through the classically described G α q-dependent pathway. Interestingly, this calcium response was biphasic with an initial intracellular ER store source followed by a CRAC-dependent, long-lasting calcium influx from the extracellular medium. This profile was not observed in CMT93 cells treated with the canonical PAR2 agonist, trypsin (Suppl. Figure S1), where the prompt increase in cytosolic calcium was immediately followed by a decrease in the calcium response never rising up afterwards. This difference in the calcium profiles was even more pronounced in renal-derived cells (HEK), that we also used to explore the pharmacology of PARs (compare Figure 6B and trypsin response seen in Kawabata *et al.* (Kawabata et al. 1999). This SOCE activation could be of importance knowing that this process may potentiate or prolongate the effects of the primary calcium response (Targos, Baranska, and Pomorski 2005).

Our data suggested that both chymotrypsin and trypsin may use the same canonical R³⁶/S³⁷ cleavage site to generate a calcium signaling *via* PAR2. Thus, the divergent calcium profiles between these enzymes are hard to explain but could be attributed either to differences in the interaction between the enzyme and PAR2 or to a concomitant action of chymotrypsin on a cell membrane target not affected by trypsin. In line with this concept, Kaiserman *et al.* showed that despite cleaving at the PAR2 canonical site, Granzyme K (GzmK) and trypsin had opposite effects, GzmK being unable to induce any calcium signaling while inducing ERK phosphorylation (Kaiserman et al. 2022). This result emphasises the complexity of proteolytic signaling mechanisms and underlines that identifying the sole PAR2 cleavage site is not sufficient to predict which downstream signaling pathways will be

activated by a protease. Furthermore, our HPLC-MS analysis identified a major cleavage site for chymotrypsin on the PAR2 N-terminus at L³⁸/I³⁹. If occurring in living cells, this cleavage does not appear to drive calcium or ERK1/2 signaling according to our results (Supp. Figure S4). However, this cleavage could represent a way to limit PAR2 activation. This hypothesis could explain the lower magnitude of the calcium response induced by chymotrypsin compared to trypsin in CMT93 cells (compare Figure 2B and Supp. Figure S1C). In the literature, the cleavage of PAR2 at the L³⁸/I³⁹ site has been reported to induce eosinophil degranulation, *via* an aspartate protease activity produced by a fungus (Matsuwaki et al. 2009). Therefore, depending on the cell context, the L³⁸/I³⁹ cleavage site on PAR2 may or may not exhibit functional effects.

Based on the existing PAR2 pharmacology literature, it appears that pancreatic chymotrypsin stands out from other proteases with chymotrypsin-like activity. Indeed, while the neutrophil protease Cathepsin G (CatG) disarms PAR2, KLK7 was unable to activate or disarm PAR2 in KNRK cells (De Bruyn et al. 2021; Stefansson et al. 2008). Chymase, another chymotrypsin-like protease, was unable to activate PAR2 in keratinocytes (Schechter et al. 1998). Therefore, a picture that emerges from literature is that chymotrypsin-like activities are generally either disarming or without effect towards PAR2. However, our study contradicts this concept. Importantly, Schechter and colleagues also found that chymotrypsin was not able to activate PAR2, a result that is opposite to ours and which highlights the importance of the cellular context.

Our work clearly demonstrates that in addition to being a PAR2 activator, chymotrypsin is a very efficient PAR1-disarming protease by cleaving the receptor 2 amino acids downstream of the canonical site, at F⁴³/L⁴⁴. This makes thrombin unable to signal *via* PAR1 anymore. Our study is in agreement with previous work, which showed that a synthetic peptide corresponding to the PAR1 N-terminal region 38-60 was cleaved at the same F⁴³/L⁴⁴ site by chymotrypsin (Parry et al. 1996). However, the functional outcome of such a cleavage occurring on the whole receptor expressed on living cells had not been evaluated. The disarming of calcium signals that we report here also provides

a functional explanation to pioneering experiments in the 1980s, which showed that platelets previously exposed to pancreatic chymotrypsin exhibited a delayed thrombin-induced aggregation (Tam, Fenton, and Detwiler 1980). Previous studies reported that cathepsin G and chymase also had the ability to disarm PAR1 (Schechter et al. 1998; De Bruyn et al. 2021; Molino et al. 1995; Renesto et al. 1997). Therefore, a PAR1 disarming effect appears to be a common characteristic of chymotrypsin-like proteases.

Interestingly, in our experiments, the IC₅₀ for PAR1 disarming by chymotrypsin was very low, i.e. 0.02 U/mL (corresponding to 12 nM), a concentration at which no effect on PAR2 is observed. Similarly, Parry and colleagues concluded that, despite a lower cleavage efficiency, the affinity of chymotrypsin for PAR1 was equivalent to that of thrombin, making PAR1 a very good chymotrypsin substrate (Parry et al. 1996). These observations suggest that, under physiological conditions, pancreatic chymotrypsin present in the lumen could disarm PAR1 well before activating PAR2. The physiological effect of this disarming remains to be elucidated, but since thrombin has been shown to be secreted in the gut lumen by IECs (Motta et al. 2019; Motta, Palese, et al. 2021; Motta, Deraison, et al. 2021), PAR1 activation and disarming actions are relevant at the apical side of the epithelium. In human organoids, PAR1 cleavage by thrombin has been associated with increased epithelial cell maturation and apoptosis (Sebert et al. 2018). In contrast, Darmoul *et al.* linked PAR1 expression with a cancerous context (Darmoul et al. 2003). The same group reported that activation of PAR1 by thrombin or its agonist peptide TFLLR drives proliferation of HT29 cells (Darmoul et al. 2004). Chymotrypsin, by disarming PAR1, could therefore have anti-apoptotic or anti-proliferative effects depending on the context (primary versus cancerous IECs). In summary, our results suggest that chymotrypsin could be a major regulator of PAR1 and PAR2 activity at the intestinal epithelium surface.

CONCLUSION

Taken together, our results clearly define chymotrypsin as a luminal protease of the gut that neighbours the colonic epithelium, where PARs are expressed. We show that in intestinal epithelial cells, chymotrypsin cleaves the extracellular domains of PAR2 and PAR1 and thereby transduces or prevents intracellular signals, respectively. Our data define a new potential role of luminal chymotrypsin as a regulator of gut epithelial signaling. Future work is thus warranted to determine the role of chymotrypsin signaling in intestinal inflammation and cancer.

References

- Adams, M. N., R. Ramachandran, M. K. Yau, J. Y. Suen, D. P. Fairlie, M. D. Hollenberg, and J. D. Hooper. 2011. 'Structure, function and pathophysiology of protease activated receptors', *Pharmacol Ther*, 130: 248-82.
- Alexander, S. P., A. Christopoulos, A. P. Davenport, E. Kelly, A. Mathie, J. A. Peters, E. L. Veale, J. F. Armstrong, E. Faccenda, S. D. Harding, A. J. Pawson, C. Southan, J. A. Davies, M. P. Abbracchio, W. Alexander, K. Al-Hosaini, M. Back, N. M. Barnes, R. Bathgate, J. M. Beaulieu, K. E. Bernstein, B. Bettler, N. J. M. Birdsall, V. Blaho, F. Boulay, C. Bousquet, H. Brauner-Osborne, G. Burnstock, G. Calo, J. P. Castano, K. J. Catt, S. Ceruti, P. Chazot, N. Chiang, B. Chini, J. Chun, A. Cianciulli, O. Civelli, L. H. Clapp, R. Couture, Z. Csaba, C. Dahlgren, G. Dent, K. D. Singh, S. D. Douglas, P. Dournaud, S. Eguchi, E. Escher, E. J. Filardo, T. Fong, M. Fumagalli, R. R. Gainetdinov, M. Gasparo, C. Gerard, M. Gershengorn, F. Gobeil, T. L. Goodfriend, C. Goudet, K. J. Gregory, A. L. Gundlach, J. Hamann, J. Hanson, R. L. Hauger, D. L. Hay, A. Heinemann, M. D. Hollenberg, N. D. Holliday, M. Horiuchi, D. Hoyer, L. Hunyady, A. Husain, I. Jzerman AP, T. Inagami, K. A. Jacobson, R. T. Jensen, R. Jockers, D. Jonnalagadda, S. Karnik, K. Kaupmann, J. Kemp, C. Kennedy, Y. Kihara, T. Kitazawa, P. Kozielowicz, H. J. Kreienkamp, J. P. Kukkonen, T. Langenhan, K. Leach, D. Lecca, J. D. Lee, S. E. Leeman, J. Leprince, X. X. Li, T. L. Williams, S. J. Lolait, A. Lupp, R. Macrae, J. Maguire, J. Mazella, C. A. McArdle, S. Melmed, M. C. Michel, L. J. Miller, V. Mitolo, B. Mouillac, C. E. Muller, P. Murphy, J. L. Nahon, T. Ngo, X. Norel, D. Nyimanu, A. M. O'Carroll, S. Offermanns, M. A. Panaro, M. Parmentier, R. G. Pertwee, J. P. Pin, E. R. Prossnitz, M. Quinn, R. Ramachandran, M. Ray, R. K. Reinscheid, P. Rondard, G. E. Rovati, C. Ruzza, G. J. Sanger, T. Schoneberg, G. Schulte, S. Schulz, D. L. Segaloff, C. N. Serhan, L. A. Stoddart, Y. Sugimoto, R. Summers, V. P. Tan, D. Thal, W. W. Thomas, Pbmwm Timmermans, K. Tirupula, G. Tulipano, H. Unal, T. Unger, C. Valant, P. Vanderheyden, D. Vaudry, H. Vaudry, J. P. Vilardaga, C. S. Walker, J. M. Wang, D. T. Ward, H. J. Wester, G. B. Willars, T. M. Woodruff, C. Yao, and R. D. Ye. 2021. 'THE CONCISE GUIDE TO PHARMACOLOGY 2021/22: G protein-coupled receptors', *Br J Pharmacol*, 178 Suppl 1: S27-S156.
- Bohm, S. K., W. Kong, D. Bromme, S. P. Smeekens, D. C. Anderson, A. Connolly, M. Kahn, N. A. Nelken, S. R. Coughlin, D. G. Payan, and N. W. Bunnnett. 1996. 'Molecular cloning, expression and potential functions of the human proteinase-activated receptor-2', *Biochem J*, 314 (Pt 3): 1009-16.
- Borgstrom, B., A. Dahlqvist, G. Lundh, and J. Sjovall. 1957. 'Studies of intestinal digestion and absorption in the human', *J Clin Invest*, 36: 1521-36.
- Buresi, M. C., E. Schleichauf, N. Vergnolle, A. Buret, J. L. Wallace, M. D. Hollenberg, and W. K. MacNaughton. 2001. 'Protease-activated receptor-1 stimulates Ca(2+)-dependent Cl(-) secretion in human intestinal epithelial cells', *Am J Physiol Gastrointest Liver Physiol*, 281: G323-32.
- Camirero, A., J. L. McCarville, H. J. Galipeau, C. Deraison, S. P. Bernier, M. Constante, C. Rolland, M. Meisel, J. A. Murray, X. B. Yu, A. Alaedini, B. K. Coombes, P. Bercik, C. M. Southward, W. Ruf, B. Jabri, F. G. Chirido, J. Casqueiro, M. G. Surette, N. Vergnolle, and E. F. Verdu. 2019. 'Duodenal bacterial proteolytic activity determines sensitivity to dietary antigen through protease-activated receptor-2', *Nat Commun*, 10: 1198.
- Canivet, C., S. Gourgou-Bourgade, B. Napoleon, L. Palazzo, N. Flori, P. Guibert, G. Piessen, D. Farges-Bancel, J. F. Seitz, E. Assenat, V. Vendrely, S. Truant, G. Vanbiervliet, P. Berthelemy, S. Garcia, A. Gomez-Brouchet, L. Buscail, B. Bournet, and Bacap Consortium. 2018. 'A prospective clinical and biological database for pancreatic adenocarcinoma: the BACAP cohort', *BMC Cancer*, 18: 986.

- Cenac, N., A. M. Coelho, C. Nguyen, S. Compton, P. Andrade-Gordon, W. K. MacNaughton, J. L. Wallace, M. D. Hollenberg, N. W. Bunnett, R. Garcia-Villar, L. Bueno, and N. Vergnolle. 2002. 'Induction of intestinal inflammation in mouse by activation of proteinase-activated receptor-2', *Am J Pathol*, 161: 1903-15.
- Chin, A. C., N. Vergnolle, W. K. MacNaughton, J. L. Wallace, M. D. Hollenberg, and A. G. Buret. 2003. 'Proteinase-activated receptor 1 activation induces epithelial apoptosis and increases intestinal permeability', *Proc Natl Acad Sci U S A*, 100: 11104-9.
- Cuffe, J. E., M. Bertog, S. Velazquez-Rocha, O. Dery, N. Bunnett, and C. Korbmacher. 2002. 'Basolateral PAR-2 receptors mediate KCl secretion and inhibition of Na⁺ absorption in the mouse distal colon', *J Physiol*, 539: 209-22.
- D'Andrea, M. R., C. K. Derian, D. Leturcq, S. M. Baker, A. Brunmark, P. Ling, A. L. Darrow, R. J. Santulli, L. F. Brass, and P. Andrade-Gordon. 1998. 'Characterization of protease-activated receptor-2 immunoreactivity in normal human tissues', *J Histochem Cytochem*, 46: 157-64.
- Darmoul, D., V. Gratio, H. Devaud, T. Lehy, and M. Laburthe. 2003. 'Aberrant expression and activation of the thrombin receptor protease-activated receptor-1 induces cell proliferation and motility in human colon cancer cells', *Am J Pathol*, 162: 1503-13.
- Darmoul, D., V. Gratio, H. Devaud, F. Peiretti, and M. Laburthe. 2004. 'Activation of proteinase-activated receptor 1 promotes human colon cancer cell proliferation through epidermal growth factor receptor transactivation', *Mol Cancer Res*, 2: 514-22.
- De Bruyn, M., H. Ceuleers, N. Hanning, M. Berg, J. G. De Man, P. Hulpiau, C. Hermans, U. H. Stenman, H. Koistinen, A. M. Lambeir, B. Y. De Winter, and I. De Meester. 2021. 'Proteolytic Cleavage of Bioactive Peptides and Protease-Activated Receptors in Acute and Post-Colitis', *Int J Mol Sci*, 22.
- Dulon, S., C. Cande, N. W. Bunnett, M. D. Hollenberg, M. Chignard, and D. Pidard. 2003. 'Proteinase-activated receptor-2 and human lung epithelial cells: disarming by neutrophil serine proteinases', *Am J Respir Cell Mol Biol*, 28: 339-46.
- Goldberg, D. M., R. Campbell, and A. D. Roy. 1968. 'Binding of trypsin and chymotrypsin by human intestinal mucosa', *Biochim Biophys Acta*, 167: 613-5.
- Goldberg, D. M. 1969. 'Fate of trypsin and chymotrypsin in the human small intestine', *Gut*, 10: 477-83.
- Hollenberg, M. D., K. Mihara, D. Polley, J. Y. Suen, A. Han, D. P. Fairlie, and R. Ramachandran. 2014. 'Biased signalling and proteinase-activated receptors (PARs): targeting inflammatory disease', *Br J Pharmacol*, 171: 1180-94.
- Holzhausen, M., L. C. Spolidorio, R. P. Ellen, M. C. Jobin, M. Steinhoff, P. Andrade-Gordon, and N. Vergnolle. 2006. 'Protease-activated receptor-2 activation: a major role in the pathogenesis of Porphyromonas gingivalis infection', *Am J Pathol*, 168: 1189-99.
- Iablokov, V., C. L. Hirota, M. A. Peplowski, R. Ramachandran, K. Mihara, M. D. Hollenberg, and W. K. MacNaughton. 2014. 'Proteinase-activated receptor 2 (PAR2) decreases apoptosis in colonic epithelial cells', *J Biol Chem*, 289: 34366-77.
- Kaiserman, D., P. Zhao, C. L. Rowe, A. Leong, N. Barlow, L. T. Joeckel, C. Hitchen, S. E. Stewart, M. D. Hollenberg, N. Bunnett, A. Suhrbier, and P. I. Bird. 2022. 'Granzyme K initiates IL-6 and IL-8 release from epithelial cells by activating protease-activated receptor 2', *PLoS One*, 17: e0270584.
- Kawabata, A., M. Saifeddine, B. Al-Ani, L. Leblond, and M. D. Hollenberg. 1999. 'Evaluation of proteinase-activated receptor-1 (PAR1) agonists and antagonists using a cultured cell receptor desensitization assay: activation of PAR2 by PAR1-targeted ligands', *J Pharmacol Exp Ther*, 288: 358-70.
- Kong, W., K. McConalogue, L. M. Khitin, M. D. Hollenberg, D. G. Payan, S. K. Bohm, and N. W. Bunnett. 1997. 'Luminal trypsin may regulate enterocytes through proteinase-activated receptor 2', *Proc Natl Acad Sci U S A*, 94: 8884-9.

- Lau, C., C. Lytle, D. S. Straus, and K. A. DeFea. 2011. 'Apical and basolateral pools of proteinase-activated receptor-2 direct distinct signaling events in the intestinal epithelium', *Am J Physiol Cell Physiol*, 300: C113-23.
- Matsuwaki, Y., K. Wada, T. A. White, L. M. Benson, M. C. Charlesworth, J. L. Checkel, Y. Inoue, K. Hotta, J. U. Ponikau, C. B. Lawrence, and H. Kita. 2009. 'Recognition of fungal protease activities induces cellular activation and eosinophil-derived neurotoxin release in human eosinophils', *J Immunol*, 183: 6708-16.
- Mihara, K., R. Ramachandran, B. Renaux, M. Saifeddine, and M. D. Hollenberg. 2013. 'Neutrophil elastase and proteinase-3 trigger G protein-biased signaling through proteinase-activated receptor-1 (PAR1)', *J Biol Chem*, 288: 32979-90.
- Mihara, K., R. Ramachandran, M. Saifeddine, K. K. Hansen, B. Renaux, D. Polley, S. Gibson, C. Vanderboor, and M. D. Hollenberg. 2016. 'Thrombin-Mediated Direct Activation of Proteinase-Activated Receptor-2: Another Target for Thrombin Signaling', *Mol Pharmacol*, 89: 606-14.
- Molino, M., N. Blanchard, E. Belmonte, A. P. Tarver, C. Abrams, J. A. Hoxie, C. Cerletti, and L. F. Brass. 1995. 'Proteolysis of the human platelet and endothelial cell thrombin receptor by neutrophil-derived cathepsin G', *J Biol Chem*, 270: 11168-75.
- Motta, J. P., A. Denadai-Souza, D. Sagnat, L. Guiraud, A. Edir, C. Bonnart, M. Sebbag, P. Rousset, A. Lapeyre, C. Seguy, N. Mathurine-Thomas, H. J. Galipeau, D. Bonnet, L. Alric, A. G. Buret, J. L. Wallace, A. Dufour, E. F. Verdu, M. D. Hollenberg, E. Oswald, M. Serino, C. Deraison, and N. Vergnolle. 2019. 'Active thrombin produced by the intestinal epithelium controls mucosal biofilms', *Nat Commun*, 10: 3224.
- Motta, J. P., C. Deraison, S. Le Grand, B. Le Grand, and N. Vergnolle. 2021. 'PAR-1 Antagonism to Promote Gut Mucosa Healing in Crohn's Disease Patients: A New Avenue for CVT120165', *Inflamm Bowel Dis*, 27: S33-S37.
- Motta, J. P., S. Palese, C. Giorgio, K. Chapman, A. Denadai-Souza, P. Rousset, D. Sagnat, L. Guiraud, A. Edir, C. Seguy, L. Alric, D. Bonnet, B. Bournet, L. Buscail, C. Gilletta, A. G. Buret, J. L. Wallace, M. D. Hollenberg, E. Oswald, E. Barocelli, S. Le Grand, B. Le Grand, C. Deraison, and N. Vergnolle. 2021. 'Increased Mucosal Thrombin is Associated with Crohn's Disease and Causes Inflammatory Damage through Protease-activated Receptors Activation', *J Crohns Colitis*, 15: 787-99.
- Nasri, I., D. Bonnet, B. Zwarycz, E. d'Aldebert, S. Khou, R. Mezghani-Jarraya, M. Quaranta, C. Rolland, C. Bonnart, E. Mas, A. Ferrand, N. Cenac, S. Magness, L. Van Landeghem, N. Vergnolle, and C. Racaud-Sultan. 2016. 'PAR2-dependent activation of GSK3beta regulates the survival of colon stem/progenitor cells', *Am J Physiol Gastrointest Liver Physiol*, 311: G221-36.
- Nguyen, C., A. M. Coelho, E. Grady, S. J. Compton, J. L. Wallace, M. D. Hollenberg, N. Cenac, R. Garcia-Villar, L. Bueno, M. Steinhoff, N. W. Bunnett, and N. Vergnolle. 2003. 'Colitis induced by proteinase-activated receptor-2 agonists is mediated by a neurogenic mechanism', *Can J Physiol Pharmacol*, 81: 920-7.
- Nystedt, S., K. Emilsson, A. K. Larsson, B. Strombeck, and J. Sundelin. 1995. 'Molecular cloning and functional expression of the gene encoding the human proteinase-activated receptor 2', *Eur J Biochem*, 232: 84-9.
- Nystedt, S., K. Emilsson, C. Wahlestedt, and J. Sundelin. 1994. 'Molecular cloning of a potential proteinase activated receptor', *Proc Natl Acad Sci U S A*, 91: 9208-12.
- Nystedt, S., A. K. Larsson, H. Aberg, and J. Sundelin. 1995. 'The mouse proteinase-activated receptor-2 cDNA and gene. Molecular cloning and functional expression', *J Biol Chem*, 270: 5950-55.
- Oikonomopoulou, K., K. K. Hansen, M. Saifeddine, I. Tea, M. Blaber, S. I. Blaber, I. Scarisbrick, P. Andrade-Gordon, G. S. Cottrell, N. W. Bunnett, E. P. Diamandis, and M. D. Hollenberg. 2006. 'Proteinase-activated receptors, targets for kallikrein signaling', *J Biol Chem*, 281: 32095-112.
- Pandol, S. J. 2010. *The Exocrine Pancreas* (San Rafael (CA)).
- Parry, M. A., T. Myles, J. Tschopp, and S. R. Stone. 1996. 'Cleavage of the thrombin receptor: identification of potential activators and inactivators', *Biochem J*, 320 (Pt 1): 335-41.

- Peach, C. J., L. E. Edgington-Mitchell, N. W. Bunnett, and B. L. Schmidt. 2023. 'Protease-activated receptors in health and disease', *Physiol Rev*, 103: 717-85.
- Ramachandran, R., C. Altier, K. Oikonomopoulou, and M. D. Hollenberg. 2016. 'Proteinases, Their Extracellular Targets, and Inflammatory Signaling', *Pharmacol Rev*, 68: 1110-42.
- Ramachandran, R., K. Mihara, H. Chung, B. Renaux, C. S. Lau, D. A. Muruve, K. A. DeFea, M. Bouvier, and M. D. Hollenberg. 2011. 'Neutrophil elastase acts as a biased agonist for proteinase-activated receptor-2 (PAR2)', *J Biol Chem*, 286: 24638-48.
- Ramachandran, R., K. Mihara, M. Mathur, M. D. Rochdi, M. Bouvier, K. Defea, and M. D. Hollenberg. 2009. 'Agonist-biased signaling via proteinase activated receptor-2: differential activation of calcium and mitogen-activated protein kinase pathways', *Mol Pharmacol*, 76: 791-801.
- Ramachandran, R., F. Noorbakhsh, K. Defea, and M. D. Hollenberg. 2012. 'Targeting proteinase-activated receptors: therapeutic potential and challenges', *Nat Rev Drug Discov*, 11: 69-86.
- Reinhardt, C., M. Bergental, T. U. Greiner, F. Schaffner, G. Ostergren-Lunden, L. C. Petersen, W. Ruf, and F. Backhed. 2012. 'Tissue factor and PAR1 promote microbiota-induced intestinal vascular remodelling', *Nature*, 483: 627-31.
- Remtulla, M. A., P. R. Durie, and D. M. Goldberg. 1986. 'Stool chymotrypsin activity measured by a spectrophotometric procedure to identify pancreatic disease in infants', *Clin Biochem*, 19: 341-7.
- Renesto, P., M. Si-Tahar, M. Moniatte, V. Balloy, A. Van Dorsselaer, D. Pidard, and M. Chignard. 1997. 'Specific inhibition of thrombin-induced cell activation by the neutrophil proteinases elastase, cathepsin G, and proteinase 3: evidence for distinct cleavage sites within the aminoterminal domain of the thrombin receptor', *Blood*, 89: 1944-53.
- Roka, R., J. Demaude, N. Cenac, L. Ferrier, C. Salvador-Cartier, R. Garcia-Villar, J. Fioramonti, and L. Bueno. 2007. 'Colonic luminal proteases activate colonocyte proteinase-activated receptor-2 and regulate paracellular permeability in mice', *Neurogastroenterol Motil*, 19: 57-65.
- Schechter, N. M., L. F. Brass, R. M. Lavker, and P. J. Jensen. 1998. 'Reaction of mast cell proteases tryptase and chymase with protease activated receptors (PARs) on keratinocytes and fibroblasts', *J Cell Physiol*, 176: 365-73.
- Sebert, M., A. Denadai-Souza, M. Quaranta, C. Racaud-Sultan, S. Chabot, P. Lluel, N. Monjotin, L. Alric, G. Portier, S. Kirzin, D. Bonnet, A. Ferrand, and N. Vergnolle. 2018. 'Thrombin modifies growth, proliferation and apoptosis of human colon organoids: a protease-activated receptor 1- and protease-activated receptor 4-dependent mechanism', *Br J Pharmacol*, 175: 3656-68.
- Sebert, M., N. Sola-Tapias, E. Mas, F. Barreau, and A. Ferrand. 2019. 'Protease-Activated Receptors in the Intestine: Focus on Inflammation and Cancer', *Front Endocrinol (Lausanne)*, 10: 717.
- Singer, M. V., and E. Niebergall-Roth. 2009. 'Secretion from acinar cells of the exocrine pancreas: role of enteropancreatic reflexes and cholecystinin', *Cell Biol Int*, 33: 1-9.
- Smith, J. S., I. Ediss, M. A. Mullinger, and A. Bogoch. 1971. 'Fecal chymotrypsin and trypsin determinations', *Can Med Assoc J*, 104: 691-4 passim.
- Stefansson, K., M. Brattsand, D. Roosterman, C. Kempkes, G. Bocheva, M. Steinhoff, and T. Egelrud. 2008. 'Activation of proteinase-activated receptor-2 by human kallikrein-related peptidases', *J Invest Dermatol*, 128: 18-25.
- Swystun, V. A., B. Renaux, F. Moreau, S. Wen, M. A. Peplowski, M. D. Hollenberg, and W. K. MacNaughton. 2009. 'Serine proteases decrease intestinal epithelial ion permeability by activation of protein kinase Czeta', *Am J Physiol Gastrointest Liver Physiol*, 297: G60-70.
- Tam, S. W., J. W. Fenton, 2nd, and T. C. Detwiler. 1980. 'Platelet thrombin receptors. Binding of alpha-thrombin is coupled to signal generation by a chymotrypsin-sensitive mechanism', *J Biol Chem*, 255: 6626-32.
- Tanaka, Y., F. Sekiguchi, H. Hong, and A. Kawabata. 2008. 'PAR2 triggers IL-8 release via MEK/ERK and PI3-kinase/Akt pathways in GI epithelial cells', *Biochem Biophys Res Commun*, 377: 622-26.
- Targos, B., J. Baranska, and P. Pomorski. 2005. 'Store-operated calcium entry in physiology and pathology of mammalian cells', *Acta Biochim Pol*, 52: 397-409.

- van der Merwe, J. Q., M. D. Hollenberg, and W. K. MacNaughton. 2008. 'EGF receptor transactivation and MAP kinase mediate proteinase-activated receptor-2-induced chloride secretion in intestinal epithelial cells', *Am J Physiol Gastrointest Liver Physiol*, 294: G441-51.
- Vergnolle, N. 2005. 'Clinical relevance of proteinase activated receptors (pars) in the gut', *Gut*, 54: 867-74.
- Vergnolle, N. 2016. 'Protease inhibition as new therapeutic strategy for GI diseases', *Gut*.

Figure Legends

Figure 1. The colonic epithelium is exposed to chymotrypsin activity. (A) Immunodetection of chymotrypsin B (CTRB) in different gut sub-compartments from mouse samples (left panel) and human samples (right panel) by Western blot. Human and murine pancreas were used as positive controls for CTRB expression (26 kDa) and murine lung was used as a negative control. Different amounts of protein extracts were loaded to adapt to different chymotrypsin abundance among the samples and to avoid signal saturation: 2 μg and 0.1 μg for human and murine pancreas, respectively; 25 μg and 17 μg for human and mouse feces, respectively; 40 μg , 50 μg and 7 μg for murine colonic scrapings, human mucus and human colonic biopsy, respectively. L : Precision plus protein ladder (Bio-Rad). Of note, aspecific signals were visible in extracts from murine lung, scraping from washed mucosa and human mucus protein. **(B)** Quantification of chymotrypsin-like activities in human and mouse gut sub-compartment samples. Mouse colonic scrapings and stools as well as human mucus and stools were extracted in native conditions and the chymotrypsin-like activities were assayed using Suc-Ala-Ala-Pro-Phe-AMC as a substrate. The extracts were incubated with or without chymostatin (500 μM), a specific chymotrypsin-like inhibitor. The initial velocity of the curves was extracted from the kinetic graphs, and the graphs represents the chymotrypsin-like activity in mU/mg protein for each sample. Each dot represents one patient or one mouse. * $p < 0.05$; ** $p < 0.01$; **** $p < 0.0001$ (Wilcoxon matched-pairs signed-rank test).

Figure 2. Chymotrypsin cleaves PAR2 and induces calcium signaling in CMT93 intestinal epithelial cells. (A) Cleavage quantification of the extracellular domain of PAR2. CHO cells stably expressing nanoLuciferase-hPAR2-YFP were incubated with increasing amount of chymotrypsin for 10 min. Luciferase activity was measured in the supernatant and divided by total luciferase activity present in untreated cells. The graph represents the mean \pm -SD of the % of released nanoLuciferase activity as a

function of chymotrypsin concentration (transformed in Log10). A curve with a standard slope (Hill slope = 1) was represented. The graph represents five independent experiments. **(B)** Calcium mobilization assays using Fluo8-loaded CMT93 cells treated with increasing amount of chymotrypsin. Injection of chymotrypsin (Chymo) was performed at time 4 seconds. The fluorescence of the calcium Fluo8 probe was recorded over 200 seconds and represents the fluorescent level normalized by the baseline level (F/baseline), which is the level of fluorescence before injection. The calcium response observed in WT CMT93, expressing PAR2 endogenously, was totally abolished in PAR2^{-/-} cells. The maximum fluorescence value (Fmax) obtained for each concentration of chymotrypsin (right panel) were compared between PAR2^{+/+} and PAR2^{-/-} cells. Each dot on the plot represents one independent experiment. *p<0.05 (Wilcoxon matched-pairs signed rank test). **(C)** Calcium mobilization assays using Fluo8-loaded CMT93 cells treated with increasing amount of chymotrypsin and the PAR2 antagonist I-191 at 10 μM. The maximum fluorescence values (Fmax) obtained with 40 U/mL chymotrypsin in the presence or not of I-191 were quantified and compared (right panel). Each dot on the plot represents one independent experiment, paired data are connected by a line. *p<0.05 (Wilcoxon matched-pairs signed-rank test).

Figure 3. Gαq proteins, but not Gα12/13 nor Gαi proteins are involved in the calcium signal downstream PAR2 activation by chymotrypsin in CMT93 cells. Calcium mobilization assay using Fluo8-loaded CMT93 cells treated with 40 U/mL chymotrypsin after pre-incubation with Gα antagonists: **(A)** YM-254890 (Gαq antagonist) at 10 μM during 5 min, **(B)** Y-27632 (Rho-dependent Gα12/13 antagonist) at 10 μM for 10 min, or **(C)** PTX (Gαi antagonist) at 100 ng/mL for 16h. Vehicles were 0.1% DMSO **(A)** or water **(B-C)**. Profiles are representative of one experiment that was repeated five independent times minimum. The Fmax obtained for each experiment was plotted on graphs (right-hand panels). *p<0.05; ns: non-significant (Wilcoxon matched-pairs signed-rank test).

Figure 4. CRAC channels are involved in the long-term calcium influx observed downstream of PAR2 activation by chymotrypsin in CMT93 cells. (A) Calcium mobilization assays of Fluo8-loaded CMT93 cells stimulated with 40 U/mL chymotrypsin. A pre-treatment of 1h was done with the intracellular calcium chelator BAPTA-AM at 30 μ M or its vehicle (0.03% DMSO). The experiment was performed six independent times and the Fmax of each experiment was reported on the right-hand graph. * $p < 0.05$ (Wilcoxon matched-pairs signed-rank test). (B) Calcium mobilization assays of Fluo8-loaded CMT93 cells stimulated with 40 U/mL chymotrypsin, in the presence or absence of extracellular calcium (-Calcium). The calcium influx occurring after the initial RE store mobilization was quantified using Area Under the Curves (AUC) from 100 to 200 sec. The graph represents AUC calculated from seven independent experiments. ** $p < 0.01$ (Wilcoxon matched-pairs signed-rank test). (C) Calcium mobilization assays of Fluo8-loaded CMT93 cells using a two-step strategy to uncouple the intracellular store mobilization from the extracellular influx. CMT93 cells were first stimulated with chymotrypsin (represented by an arrow) in calcium-free conditions (0 mM Ca^{2+}). The experiment was done in the presence or absence of the CRAC antagonist BTP2 at 10 μ M or its vehicle (0.04% DMSO). Then, 240 seconds after the first stimulation, a CaCl_2 solution was added (2 mM Ca^{2+} final concentration). Curves show the results of one representative experiment repeated five independent times. Calcium influx was quantified by measuring the AUC following CaCl_2 injection (240-350 sec). * $p < 0.05$ (Wilcoxon matched-pairs signed-rank test).

Figure 5. Chymotrypsin activates ERK1/2 signaling pathway *via* PAR2, depending on G α q and G α i proteins in intestinal epithelial cells. (A) Representative immunoblots of ERK1/2 phosphorylation in WT (PAR2^{+/+}) or PAR2^{-/-} CMT93 cells. Cells were treated for 10 min with increasing concentrations of chymotrypsin (0 – 20 U/mL). Heat-inactivated chymotrypsin (20 U/mL) was used as control (Δ 20). Cell lysates were analysed by Western blot using anti-Phospho ERK1/2 (P-ERK) antibodies and then anti-total ERK1/2 antibodies. The ratios between P-ERK and total ERK signals were quantified by

densitometric analysis and represented on the graph below the blots. Each dot on the plot represents one independent experiment. * $p < 0.05$ (Wilcoxon matched-pairs signed-rank test). **(B)** ERK1/2 phosphorylation analysed by WB in WT CMT93 cells stimulated for 10 minutes with 5 U/mL chymotrypsin after pre-incubation with G α antagonists: YM-254890 at 10 μ M during 5 min, Y-27632 at 10 μ M for 10 min, or PTX at 100 ng/mL for 16h. Pre-incubations with the corresponding vehicle solutions (0.1% DMSO for YM-254890 or water for Y-27632 and PTX) served as controls. The ratios between P-ERK and total ERK signals were quantified by densitometric analysis and represented on the right-hand panels. Each dot on the plot represents one independent experiment. * $p < 0.05$ (Wilcoxon test for single comparison (effect of YM-254890); Friedman followed by the Dunn's test for multiple comparisons (effects of Y-27632 or PTX)).

Figure 6. Chymotrypsin cleaves PAR2 at L³⁸/I³⁹ site *in vitro* but the canonical R³⁶/S³⁷ site may drive calcium signaling *in cellulo*. **(A)** Determination of the cleavage sites of hPAR2 by chymotrypsin. The human PAR2 N-terminus derived peptide was incubated with chymotrypsin 5 U/mL at 37°C for 30 min and the samples were fractionated by HPLC followed by MALDI/MS. The HPLC tracing indicates the presence of a cleavage site after L³⁸ and generating the IGKVDGTSHTGKGVN-NH₂ peptide (arrowhead). The sequence of the tethered ligand is underlined. **(B)** Calcium mobilization assay of Fluo4-loaded WT HEK cells (expressing PAR1 and PAR2) or PAR2^{-/-} HEK cells stimulated with chymotrypsin 5 U/mL. **(C)** Calcium mobilization assay performed on double deficient PAR1^{-/-} and PAR2^{-/-} HEK cells stably transfected with a vector encoding mutant hPAR2 (carrying a mutation at a canonical site (R³⁶G)). Cells were stimulated with 5 U/mL chymotrypsin (left panel) or trypsin (right panel) and then by PAR2 agonist peptide 2fLI (1 μ M) as a positive control. The data in each panel are representative of five or more independent experiments.

Figure 7. Chymotrypsin cleaves PAR1 N-terminal extremity. (A) Cleavage quantification of the N-terminal domain of PAR1. CHO cells stably transfected with nLuciferase-hPAR1-YFP were incubated for 10 min with increasing amounts of chymotrypsin (0 to 10 U/mL). Luciferase activity was measured in the supernatant and divided by total luciferase activity of the cells. The graph represents the mean \pm SD of the % of released nanoLuciferase activity as a function of chymotrypsin concentration (transformed in Log10). A curve with a standard slope (Hill slope = 1) was represented. The graph represents five independent experiments. **(B)** Determination of the cleavage sites of hPAR1 by chymotrypsin. The human PAR1 N-terminus-derived peptide was incubated in the absence (-chymotrypsin) or presence of chymotrypsin 5 U/mL (+ chymotrypsin) for 30 min at 37°C and the samples were fractionated by HPLC followed by MALDI/MS. HPLC/MS analysis indicates the presence of 2 peptides derived from the full-length parental peptide (arrowheads), and reveals a unique and unambiguous cleavage site after F⁴³, 2 amino acids after the canonical cleavage site. The sequence of the tethered ligand is underlined. The profile is representative of five or more experiments.

Figure 8. Chymotrypsin disarms PAR1 in intestinal epithelial cells. (A) Calcium flow experiments performed in Fluo8-loaded PAR2^{-/-} CMT93 cells (expressing PAR1 endogenously). Cells were stimulated with 10 U/mL thrombin (Thr) with or without the PAR1 antagonist F16357 at 100 μ M. Vehicle (veh): 0.5% DMSO. The maximum fluorescence value (Fmax) obtained with thrombin \pm F16357 for each experiment was reported on the right-hand graph. *p<0.05 (Wilcoxon matched-pairs signed-rank test). **(B)** Experimental design of PAR1 disarming experiments. Fluo8-loaded PAR2^{-/-} CMT93 cells were first treated with chymotrypsin or its vehicle (1). Five minutes later, the cell supernatant was replaced by HBSS and the recording of calcium signal started. A second stimulation (2) was performed with 10 U/mL thrombin or 25 μ M PAR1-activating peptide (TFLLR) and the calcium signal was recorded during 60 seconds. **(C)** Representative calcium response curves of PAR1 disarming by chymotrypsin (blue line) and desensitization by thrombin in PAR2^{-/-} CMT93 (orange line). **(D)** Quantification of

thrombin-induced PAR1 desensitization. The Fmax values were quantified and reported on the graph. * $p < 0.05$ (Wilcoxon matched-pairs signed-rank test). **(E)** Quantification of the chymotrypsin-induced PAR1 disarming effect. PAR2^{-/-} CMT93 cells were pre-incubated with increasing amount of chymotrypsin and then stimulated with thrombin during calcium mobilization assays as explained in (B). The Fmax induced by thrombin after incubation with chymotrypsin was compared to the value obtained with thrombin alone and expressed in %. * $p < 0.05$; ** $p < 0.005$; *** $p < 0.001$ (Kruskal-Wallis followed by the Dunn's test). **(F)** Concentration-response curve of PAR1 disarming by chymotrypsin in PAR2^{-/-} CMT93. The Y axis represents the percentage of the response induced by thrombin alone. The curve was generated after log-transformation of the chymotrypsin concentrations, followed by a non-linear regression for normalized responses with a standard Hill slope fixed at -1. The calculated IC50 was 0.020 U/mL with a 95% confidence interval of [0.013; 0.030]. **(G)** Representative calcium response curves of Fluo8-loaded PAR2^{-/-} CMT93 cells pre-treated or not with 10 U/ml chymotrypsin and then stimulated with the PAR1 agonist peptide TFLLR (25 μ M) as described in (B). The Fmax obtained with TFLLR after pre-incubation or not with chymotrypsin was reported on the right-hand graph. * $p < 0.05$ (Wilcoxon matched-pairs signed-rank test). Each panel represents five or more independent experiments.

Figure 9. Schematic representation of chymotrypsin interactions with PAR1 and PAR2 at the surface of intestinal epithelial cells CMT93. Pancreatic chymotrypsin is able to cleave both PAR1 and PAR2. *In vitro*, the cleavage of PAR2 by chymotrypsin occurs at an atypical site (L³⁸/I³⁹) located within the tethered ligand sequence (dark arrow). However, in a cell context, this protease might use the PAR2 canonical R³⁶/S³⁷ cleavage site to trigger calcium signaling and ERK1/2 phosphorylation (blue arrow). The ERK activation is partially mediated by G α q and G α i proteins, whereas calcium signaling is fully dependent on G α q. This calcium mobilization is composed of an initial ER store release followed by a long-lasting CRAC activation (Ca²⁺ Release-Activated Ca²⁺ Channel), enabling calcium entry from the extracellular medium. Conversely, chymotrypsin disarms PAR1 for further activation by its canonical activator thrombin by cleaving within the PAR1 tethered ligand at the F⁴³/L⁴⁴ bond (dark arrow).

*Adapted from "Activation of Protein Kinase C (PKC)", by BioRender.com (2022). Retrieved from
(Publication License: NN2566RCT9)*